Research Paper

GEOSPHERE

GEOSPHERE, v. 15

https://doi.org/10.1130/GES01652.1

14 figures; 1 table; 1 set of supplemental files

CORRESPONDENCE: fungm3@rpi.edu; meganfung@gmail.com

CITATION: Fung, M.K., Katz, M.E., Miller, K.G., Browning, J.V., and Rosenthal, Y., 2019, Sequence stratigraphy, micropaleontology, and foraminiferal geochemistry, Bass River, New Jersey paleoshelf, USA: Implications for Eocene ice-volume changes: Geosphere, v. 15, no. 0, p. 1–31, https://doi.org/10.1130/GES01652.1.

Science Editor: Raymond M. Russo
Associate Editor: Cinzia Cervato

Received 21 December 2017
Revision received 11 October 2018
Accepted 9 January 2019

Sequence stratigraphy, micropaleontology, and foraminiferal geochemistry, Bass River, New Jersey paleoshelf, USA: Implications for Eocene ice-volume changes

Megan K. Fung[1], Miriam E. Katz[1], Kenneth G. Miller[2], James V. Browning[2], and Yair Rosenthal[2,3]

[1]Department of Earth and Environmental Sciences, Rensselaer Polytechnic Institute, 110 8th Street, Troy, New York 12180, USA
[2]Department of Earth and Planetary Sciences, Rutgers University, 610 Taylor Road, Piscataway, New Jersey 08854, USA
[3]Institute of Marine and Coastal Sciences, Rutgers University, 71 Dudley Road, New Brunswick, New Jersey 08901, USA

ABSTRACT

Micropaleontological faunal studies coupled with foraminiferal geochemical analyses from the Bass River Site (Ocean Drilling Program [ODP] Leg 174AX; New Jersey, USA) reveal rapid changes in relative sea level due to million-year-scale glaciations during the early to middle Eocene, a time previously thought to have been mainly ice free. We examine benthic foraminiferal assemblages, stable isotopes ($\delta^{18}O$ and $\delta^{13}C$), Mg/Ca, planktonic foraminiferal abundances, and ostracod abundances in eight lower to middle Eocene sequences at Bass River to reconstruct paleo–water depth and paleoceanographic changes within a sequence stratigraphic framework on the New Jersey paleo–continental shelf. Distinct benthic foraminiferal biofacies are identified and interpreted for paleodepth and environmental changes. Certain dominant species (e.g., *Uvigerina* spp., *Cibicidoides eocaenus*, *Spiroplectammina alabamensis*, *Siphonina claibornensis*, and *Cibicidoides pippeni*) indicate changes in water depth and/or environmental conditions. We estimate middle to outer neritic (50–100+ m) paleodepths for much of the early to middle Eocene, with maximum water depths (~150 ± 25 m) occurring in the early Eocene. We integrate these results with ostracod abundances and diversity, planktonic foraminiferal abundances, lithofacies, downhole logs, and core erosional surfaces to create a sequence framework for the early Eocene to early late Eocene of the New Jersey coastal plain. We compare the relationships among these sequences to foraminiferal biofacies of coreholes of the New Jersey Coastal Plain Drilling Project (Island Beach, Atlantic City, and ACGS#4), showing coeval hiatuses associated with regional base-level lowerings. Benthic and planktonic foraminifera $\delta^{18}O$ coupled with low-resolution Mg/Ca measurements provide a first-order correlation of sequence boundaries and $\delta^{18}O_{seawater}$ variations, indicating glacioeustatic changes associated with the growth and decay of small ice sheets on the order of 20–30 m sea-level equivalent during the Eocene.

INTRODUCTION

The cause of eustatic changes has been widely debated (e.g., Moucha et al., 2008). Global mean sea level (GMSL) is controlled by fluctuations in either the ocean basin size or the volume of water in the ocean (e.g., Miller et al., 2005a), whereas relative sea level (RSL) is described by changes in accommodation space due to changes in (1) GMSL and/or (2) subsidence and/or uplift (Posamentier and Vail, 1988). The growth and decay of continental ice sheets produces rapid and large-scale changes in the volume of water (up to 40 m/k.y. and 200 m respectively), whereas water temperature and variations in groundwater and lake storage occur at high rates (10 m/k.y.) yet low amplitudes (~5–10 m) (e.g., Miller et al., 2005a). Fluctuations in ocean basin volume are controlled by slow (>1 m.y.) variations in sea-floor spreading rates, sedimentation, and continental collision (e.g., Miller et al., 2005a). Therefore, the only known mechanism that can explain large (>25 m) and rapid (<1 m.y.) changes in GMSL is the growth and decay of ice sheets (glacioeustasy).

Glacioeustasy in a Greenhouse World

The onset of continent-wide Antarctic glaciation occurred around the Eocene-Oligocene transition (EOT) and is marked by a prominent $\delta^{18}O$ increase at 34–33.5 Ma (e.g., Kennett and Shackleton, 1976; Miller et al., 1991, 2008; Zachos et al., 1996; Coxall et al., 2005; Katz et al., 2008; Lear et al., 2008; Carter et al., 2017). The EOT is associated with a fall of atmospheric CO_2 (e.g., DeConto and Pollard, 2003a; Pearson et al., 2009; Pagani et al., 2005, 2011) and/or a change in ocean circulation (e.g., Exon et al., 2004; Stickley et al., 2004; Scher and Martin, 2006; Livermore et al., 2007; Borrelli et al., 2014). In the first scenario, cooling caused by falling pCO_2 allowed snow to accumulate and ice sheets to expand over Antarctica at high elevations (e.g., DeConto and Pollard, 2003a). In the second scenario, the opening of two gateways resulted in the development of the Antarctic Circumpolar Current (ACC) and led to Antarctic glaciation: (1) the Drake Passage, which isolated Antarctica from South America (Scher and Martin, 2006; Livermore et al., 2007); and (2) the Tasman Rise, which isolated Antarctica from Australia (Exon et al., 2004; Stickley et al., 2004).

Although there is a consensus for the glaciation of much, if not all, of the Antarctic continent in the Oligocene, the period leading up to Antarctic glaciation remains poorly constrained. The overall cooling trend that led to the EOT began following the sustained warming period of the Early Eocene

Climatic Optimum (EECO; 52–50 Ma; Zachos et al., 2001). The Middle Eocene Climatic Optimum (MECO; ca. 41.5 Ma) is the last global warming event that occurred before the initiation of large-scale Antarctic glaciation, and is marked by a record of transient decrease in global $\delta^{18}O$ superimposed on the overall cooling trend (e.g., Bohaty and Zachos, 2003; Villa et al., 2013). Therefore, the role of glacioeustasy in a greenhouse world remains controversial, with the possibility of ice sheets in the Paleocene and middle to late Eocene dubbed the "doubthouse world" (Miller et al., 1991). This time period differs from the established Oligocene to Holocene "icehouse world," when glacioeustatic changes clearly occurred, and the Cretaceous to early Eocene "greenhouse world," which apparently lacked large-scale ice sheets (e.g., Miller et al., 2005a, 2005b).

Numerous studies provide evidence that Antarctic glaciation began prior to the EOT (e.g., Barker et al., 2007), though the extent of these glaciations and their attendant sea-level changes are poorly known. Scher et al. (2014) produced a high-resolution benthic foraminiferal $\delta^{18}O$ record in the Southern Ocean that shows a transient rise at ca. 37.3 Ma, suggesting cooling and/or ice-sheet growth prior to the EOT. Evidence of ice-rafted debris (IRD) and widespread glacier calving was found in Antarctica 2.5 m.y. prior to the EOT event (Carter et al., 2017). Starting in the late middle Eocene (43–42 Ma), increases in both planktonic and benthic $\delta^{18}O$ values occur across hiatuses, suggesting the initiation of the first ice sheet on Antarctica and the start of the incipient "icehouse world"; however, a connection to large ice sheets is uncertain due to limited isotopic evidence (Browning et al., 1996). Although the early Eocene generally has been thought to have lacked significant ice sheets, Haq et al. (1987) found numerous early Eocene sequence boundaries and corresponding falls in sea level. On the New Jersey coastal plain (northeastern USA), Browning et al. (1996) found that early Eocene (56–52 Ma) hiatuses from onshore sequences did not correspond with global $\delta^{18}O$ changes and therefore were unlikely to have been due to glacioeustasy, though the $\delta^{18}O$ data were limited and the expected change in $\delta^{18}O$ is small (e.g., 0.2‰–0.3‰ for 25 m).

Sequence Stratigraphic, Micropaleontological, and Geochemical Constraints

The use of sequence stratigraphy allows the stratigraphic record to be divided into unconformity-bounded units termed sequences (Van Wagoner et al., 1988). Sequences are bounded above and below by unconformities or their correlative surfaces (Vail et al., 1977) and are the building blocks of sequence stratigraphy. Passive continental margin sequences develop as the result of the interplay of several processes including tectonics and changes in sediment supply (e.g., Vail et al., 1977, 1991; Haq et al., 1987; Weimer and Posamentier, 1993; Christie-Blick and Driscoll, 1995; Moucha et al., 2008). By integrating lithologic, paleontologic, seismic stratigraphic, and well-log data, sequences can be identified (Browning et al., 1997a).

Benthic foraminiferal biofacies can be used as indicators of water-depth changes throughout a section, providing critical information for sequence stratigraphic interpretations. Benthic foraminifera have been widely used to evaluate paleobathymetric changes (e.g., Natland, 1933; Bandy, 1960; van Morkhoven et al., 1986; Sen Gupta, 1999) because benthic foraminiferal shelf species are immediately affected by environmental factors (i.e., food, oxygen) that change with depth. Certain benthic foraminifera inhabit specific water depths and tolerate specific environmental conditions, and therefore changes in biofacies can be used to interpret fluctuations in water depth and identify environmental changes (e.g., Douglas, 1979; Poag, 1981; Culver, 1988).

The ratio of planktonic to total foraminifera (% planktonics) is used to further aid in paleo–water depth interpretations. The percentage of planktonic foraminiferal specimens is characteristically low across the inner and middle shelf and increases rapidly across the outer shelf and upper slope; therefore, higher planktonic foraminiferal abundances typically indicate deeper water depths (e.g., Grimsdale and van Morkhoven, 1955; Gibson, 1989; van der Zwaan et al., 1990; Leckie and Olson, 2003). More specifically, percent planktonics from multiple depth transects show a typical increase from 20%–60% planktonics at 100 m to 60%–90% by 200 m (Gibson, 1989). Percent planktonics is assessed in conjunction with benthic assemblages and lithology to reconstruct paleodepth, as percent planktonics can be strongly distorted by taphonomy and dissolution (van de Zwaan et al., 1990).

Ostracod abundance and diversity can further aid in paleobathymetric and paleoenvironmental interpretations (Frenzel and Boomer, 2005). Ostracods are more sensitive to changes in temperature and oxygen conditions than benthic foraminifera (Passlow, 1997; Yasuhara et al., 2012), and as such, can provide valuable additional information to supplement the foraminiferal interpretations. In addition to reconstructing paleo–water depth from benthic foraminiferal biofacies, combined benthic foraminiferal $\delta^{18}O$ and Mg/Ca studies can provide an independent method for evaluating changes in sea level (e.g., Cramer et al., 2011; Katz et al., 2008; Lear et al., 2000, 2008). Mg/Ca analyses provide a temperature proxy, whereas $\delta^{18}O_{benthic}$ is influenced by both water temperature and $\delta^{18}O_{sw}$ (sw—seawater) changes due to ice-volume fluctuations; when combined, benthic foraminiferal $\delta^{18}O$ and Mg/Ca can be used to produce $\delta^{18}O_{sw}$ (hence sea-level) reconstructions (e.g., Lear et al., 2000, 2008).

Providing a stable-isotope and temperature record within a sequence stratigraphic framework at Bass River (New Jersey) allows us to assess the evidence of glacial growth and decay during the Eocene, prior to the onset of large-scale Antarctic glaciation at the EOT. In this paper, new micropaleontological data (benthic foraminiferal and ostracod assemblages and planktonic foraminiferal abundances) and foraminiferal geochemical analyses ($\delta^{18}O$, $\delta^{13}C$, and Mg/Ca) are integrated with lithology and previously defined New Jersey coastal plain sequences. Our first goal is to establish a more comprehensive picture of sea-level changes that occurred on the New Jersey paleo–continental shelf in the early Eocene to early late Eocene. Our second goal is to determine whether increases in $\delta^{18}O$ across sequence boundaries were associated with glacial interactions in the early to middle Eocene, a time previously believed to have been mainly ice free (e.g., Miller et al., 2005a; Harris et al., 2010).

BACKGROUND

New Jersey Sequence Stratigraphic Studies

The mid-Atlantic U.S. continental margin is an ideal setting to study changes in paleo–water depth and sequence stratigraphy because it is an old passive margin with reasonably uniform, slow subsidence (Miller and Mountain, 1994; Kominz et al., 1998). Tectonic complications due to non-thermal effects impact this margin (e.g., Moucha et al., 2008; Rowley et al., 2013), though these effects appear mostly on the >1 m.y. scale (Miller et al., 2011). Consequently, the New Jersey passive continental margin provides an exceptional record of relative sea-level change (e.g., Olsson and Wise, 1987; Miller et al., 2005a).

The extraction of inferred eustatic records from passive-margin sequences was led by the innovative work of the Exxon Production Research (EPR) Company whose work utilized seismic reflection profiles and, later, outcrops and well data (Vail et al., 1977; Haq et al., 1987; Posamentier et al., 1988). Subsequently, numerous studies have focused on Eocene sequence stratigraphy on the New Jersey coastal plain and related it to this inferred record of GMSL, finding similar timing, but major differences in amplitudes, of events.

New Jersey coastal plain sections include the lower Eocene Manasquan Formation and middle Eocene Shark River Formation in outcrop (Enright, 1969) and the subsurface (e.g., ACGS#4 corehole: Owens et al., 1988; Ocean Drilling Program [ODP] Leg 150X coreholes, Browning et al., 1996; Fig. 1). Olsson and Wise (1987) utilized foraminiferal biofacies analysis and lithofacies changes in the upper Paleocene and lower Eocene New Jersey coastal plain to recognize depositional sequences that were correlated to the original Haq et al. (1987) cycle chart, showing that foraminiferal biofacies showed similar timing of sea-level changes. However, the water-depth changes of Olsson and Wise (1987) contrast with the much higher sea-level variations (>100 m changes) of Vail et al. (1977) and Haq et al. (1987). Nonetheless, Olsson and Wise (1987) concluded that relative sea level in the late Paleocene–early Eocene was between 55 m and 120 m above present sea level.

Browning et al. (1997a) provided a comprehensive study examining the relationship of lower to middle Eocene benthic foraminiferal biofacies to sequences from four New Jersey coastal plain boreholes (Island Beach, ACGS#4, Atlantic City, and Allaire; Fig. 1), showing a similar number and pattern to the inferred GMSL curve of Haq et al. (1987). Harris et al. (2010) and Stassen et al. (2015) provided benthic foraminiferal paleodepth estimates spanning the Paleocene-Eocene boundary in New Jersey.

These previous studies of water-depth changes did not account for the effects of compaction, sediment loading, and thermal subsidence, and therefore are not a direct measure of GMSL. Backstripping, a method that progressively accounts for these effects, provides a measure of GMSL and non-tectonic subsidence (e.g., Kominz et al., 2008). Backstripping the continental margins of New Jersey (Miller et al., 2005a; Kominz et al., 2008) and Australia (John et al., 2004, 2011) yields GMSL estimates that appear to be no more than half the amplitude of the EPR sea-level curves.

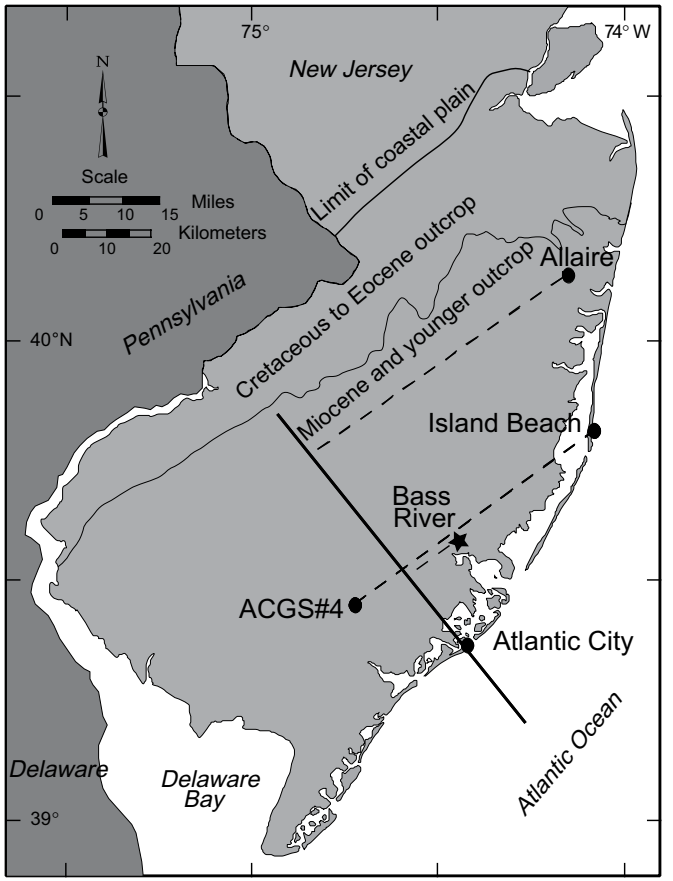

Figure 1. Location map showing Ocean Drilling Program–International Ocean Drilling Project boreholes on the New Jersey coastal plain (USA) discussed in this study. A dip profile is drawn through the Atlantic City borehole, and projections from the Bass River, ACGS#4, and Island Beach boreholes are shown. After Browning et al. (1997a).

Bass River Site

The Eocene section at Bass River (ODP Leg 174AX; Miller et al., 1998b) (Fig. 1) is the most downdip and potentially most complete of the coreholes that sample the lower Eocene to lower middle Eocene (Fig. 1; the Atlantic City corehole did not penetrate below the upper middle Eocene). The post–Paleocene-Eocene Thermal Maximum Eocene section at Bass River had not been studied in detail prior to this study. The Eocene at Bass River consists mainly of clays deposited in middle to outer neritic (30–200 m) paleodepths (Miller et al., 1998b). The Bass River samples used for this study span the lower Eocene

to lower upper Eocene (sequences E2–E10, ca. 53 Ma to ca. 37 Ma [converted to time scale of Gradstein et al., 2012]; Browning et al., 1997b). Lithostratigraphic and preliminary sequence stratigraphic interpretations (e.g., correlations of sequences E1, E2, etc.) for Bass River are previously defined in the Bass River site report (Miller et al., 1998b). The Manasquan Formation contains lower Eocene sequences E1–E4 and is composed of bioturbated silty clays with less glauconite than the overlying Shark River Formation (Miller et al., 1998b). The middle Eocene Shark River Formation (sequences E5–E9) can be further divided into a more carbonate-rich (marly) lower unit assigned to the lower Shark River Formation (sequences E5–E7) and a coarser-grained, more glauconitic upper unit assigned to the upper Shark River Formation (sequences E8–E9) (Browning et al., 1997b; Miller et al., 1998b). Previous backstripping studies of the Bass River and other Eocene coastal plain coreholes provide an estimate of GMSL changes (Kominz et al., 2008), though paleodepth estimates from Bass River used in these efforts were based on semiquantitative evaluation of widely spaced samples.

METHODS

Sequence Stratigraphic Studies

Benthic foraminiferal assemblage changes can help in interpretation of systems tracts within sequences. Systems tracts are linked depositional systems (Brown and Fisher, 1977) that are used to subdivide sequences into lowstand (LST), transgressive (TST), and highstand systems tracts (HST) (Vail, 1987; Van Wagoner et al., 1987; Posamentier and Vail, 1988; Posamentier et al., 1988). The boundary separating the LST from the overlying TST is called a transgressive surface (TS), and the surface separating the TST from the overlying HST is termed the maximum flooding surface (MFS). Where present, the LST overlies the sequence boundary (SB). When the LST is absent, as is in most New Jersey coastal plain sections, the TST may overlie the SB. A SB is recognized by an unconformity updip (commonly marked by subaerial exposure and erosion), a correlative surface downdip, and basinward shift of facies (Van Wagoner et al., 1988). Systems tracts depositional models have wide applicability and have been utilized in sequence interpretations (e.g., Abbott and Carter, 1994; Winn et al., 1995; Abreu and Anderson, 1998).

Benthic foraminifera are used to reconstruct paleobathymetry (described below), providing the means to determine shallowing- or deepening-upward trends within a sequence; this is key to distinguishing systems tracts in shelfal environments deposited below storm wave base (e.g., Gräfe, 1999; Browning et al., 1997a; Miller et al., 1998a; Pekar and Kominz, 2001; Leckie and Olson, 2003). During a regression (basinward movement of the shoreline), shallower benthic foraminiferal assemblages are deposited above deeper assemblages as the water depth decreases. In general, a LST should shallow upward as a result of progradation or exhibit relatively constant water depths due to aggradation (Posamentier et al., 1988; Neal and Abreu, 2009). Because of the shallow-water setting, LSTs are thin (<1 m) or absent in typical New Jersey coastal plain sequences; instead, the lower portions of sequences generally are characterized by a merging of the TS and sequence boundary (Browning et al., 1997b). The TSTs, which generally have common to high abundances of glauconite in New Jersey Eocene sequences (Browning et al., 1997b), show a deepening-upward trend that is characteristic of transgression. The MFS, which separates the deepening-upward TST from the shallowing-upward HST, forms in the deepest water depth of the sequence and indicates the time of the landwardmost extent of the shoreline. In a shelfal environment, the MFS is commonly associated with a condensed interval (Posamentier et al., 1988) that commonly includes the highest diversity and abundance of planktonic foraminifera and a high abundance of the genus *Uvigerina* (e.g., Loutit et al., 1988) and other infaunal taxa such as *Neobulimina* (Elderbak and Leckie, 2016). These condensed intervals of sediment starvation and high levels of glauconite typify low-oxygen middle neritic (30–100 m) and deeper paleoenvironments (Pekar et al., 2003).

Foraminiferal Studies

Foraminifera are the most abundant and well-preserved microfossils that occur regularly at Bass River and are used to reconstruct paleobathymetry. The paleodepth history of a site can be tracked through changes in important depth-indicator species (e.g., Natland, 1933; Bandy, 1960; Douglas, 1979; Olsson and Wise, 1987; Pekar et al., 1997; Sen Gupta, 1999; Leckie and Olson, 2003; Katz et al., 2003a, 2013) and percent planktonics (Grimsdale and van Morkhoven, 1955). In this study, bathymetric zonations are split into the inner neritic (0–30 m), middle neritic (30–100 m), outer neritic (100–200 m), and upper bathyal (200–600 m; van Morkhoven et al., 1986).

Samples from Bass River were taken approximately every 1.5 m (5 ft), and every 0.5 m (1.6 ft) in stratigraphically significant intervals (e.g., near sequence boundaries). In total, 43 samples were obtained for micropaleontological analyses. Samples were soaked overnight in a sodium metaphosphate solution made with deionized water (5.5 g/l), washed with tap water through a 63 µm sieve, and then oven dried at ~50 °C overnight. A microsplitter was used to obtain splits of between 149 and 369 benthic foraminiferal specimens for quantitative analysis. The ~200 specimens per sample in our shallow New Jersey margin study differs from deep-sea methods (>300 specimens), with previous studies reporting analyses with methods using counts as few as 100 specimens (e.g., Katz and Miller, 1991; Streeter and Lavery, 1982; Christensen et al., 1995). Furthermore, comparison of <200 counts versus >300 counts from multiple samples in our section shows no difference in dominant species (see Table S1 in the Supplemental Information[1]). The average number of species (species richness) for our data set is 27, compared to 55 species from middle Eocene deep-sea ODP Site 690 in the Weddell Sea, Antarctica (Thomas, 1990). This explicitly demonstrates that our diversity is lower than at deep-sea sites and validates our method of counting 200 specimens.

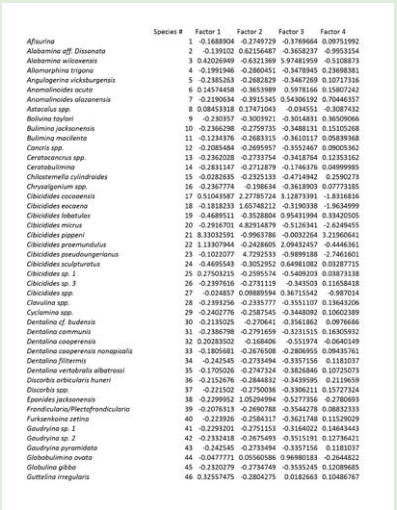

	Species #	Factor 1	Factor 2	Factor 3	Factor 4
Afiaurina	1	-0.1688904	-0.2749729	-0.3769664	0.09751992
Alabamina aff. Dissonata	2	-0.139102	0.62156487	-0.3658237	-0.0953154
Alabamina wilcoxensis	3	0.42026949	-0.6321369	5.97481959	-0.5108873
Allomorphina trigona	4	-0.1991946	-0.2860451	-0.3478945	0.23698381
Angulogerina vicksburgensis	5	-0.2385263	-0.2682829	-0.3447269	0.10717316
Anomalinoides acuta	6	0.14574458	-0.3653989	0.5978166	0.15807242
Anomalinoides alazonensis	7	-0.2190634	-0.3915345	0.54306192	0.70446357
Astacolus spp.	8	0.08453318	0.17471043	-0.034551	-0.3087432
Bolivina taylori	9	-0.230357	-0.3003921	-0.3014831	0.36509066
Bulimina jacksonensis	10	-0.2366298	-0.2759735	-0.3488131	0.15105268
Bulimina macilenta	11	-0.1234376	-0.2683315	-0.3610117	0.05839368
Cancris spp.	12	-0.2085484	-0.2695957	-0.3552467	0.09005362
Ceratocancrus spp.	13	-0.2362028	-0.2733754	-0.3418764	0.12353162
Ceratobulimina	14	-0.2831147	-0.2712879	-0.1746376	0.04999985
Chilostomella cylindroides	15	-0.0282635	-0.2325133	-0.4714942	0.2590273
Chrysalgonium spp.	16	-0.2367774	-0.198634	-0.3618903	0.07773185
Cibicidides cocoaensis	17	0.51043587	2.27785724	3.12873391	-1.8316816
Cibicidides eocaena	18	-0.1818233	1.65748212	-0.3190338	-1.9634999
Cibicidides lobatulus	19	-0.4689511	-0.3528804	0.95431994	0.33420505
Cibicidides micrus	20	-0.2916701	4.82914879	-0.5126341	-2.6249455
Cibicidides pippeni	21	8.33032591	-0.8963786	-0.0032264	3.21960641
Cibicidides praemundulus	22	1.13307944	-0.2428605	2.09432457	-0.4446361
Cibicidides pseudoungerianus	23	-0.1022077	4.7292533	-0.9899188	-2.7461601
Cibicidides sculpturatus	24	-0.4695543	-0.3052952	0.64981082	0.03287715
Cibicidides sp. 1	25	0.2750215	-0.2595574	-0.5409203	0.03873138
Cibicidides sp. 3	26	-0.2397616	-0.2731119	-0.343503	0.11658418
Cibicidides spp.	27	-0.024857	0.09889594	0.36715542	-0.987014
Clavulina spp.	28	-0.2393256	-0.2335777	-0.3551107	0.13643206
Cyclamina spp.	29	-0.2402776	-0.2587545	-0.3448092	0.10602389
Dentalina cf. budensis	30	-0.2135025	-0.270641	-0.3561862	0.0976686
Dentalina communis	31	-0.2386798	-0.2791659	-0.3231515	0.16305932
Dentalina cooperensis	32	0.20283502	-0.168406	-0.551974	-0.0640149
Dentalina cooperensis nonapicalis	33	-0.1805681	-0.2676508	-0.2806955	0.09435761
Dentalina filiformis	34	-0.242545	-0.2733494	-0.3357156	0.1181037
Dentalina vertebralis albatrossi	35	-0.1705026	-0.2747324	-0.3826846	0.10725073
Discorbis orbicularis huneri	36	-0.2152676	-0.2844832	-0.3439595	0.2119659
Discorbis spp.	37	-0.221502	-0.2750036	-0.3306211	0.15727324
Eponides jacksonensis	38	-0.2299952	1.05254994	-0.5277356	-0.2780693
Frondicularia/Plectofrondicularia	39	-0.2076313	-0.2690788	-0.3544278	0.08832333
Furkenkoina zetina	40	-0.223926	-0.2584317	-0.3621748	0.11529029
Gaudryina sp. 1	41	-0.2293201	-0.2751153	-0.3164022	0.14643443
Gaudryina sp. 2	42	-0.2332418	-0.2675493	-0.3515191	0.12736421
Gaudryina pyramidata	43	-0.242545	-0.2733494	-0.3357156	0.1181037
Globobulimina ovata	44	-0.0477771	0.05560586	0.96980183	-0.2644822
Globulina gibba	45	-0.2320279	-0.2734749	-0.3535245	0.12089685
Guttelina irregularis	46	0.32557475	-0.2804275	0.0182663	0.10486767

[1]Supplemental Information. Table S1 includes counts of all identified benthic foraminiferal species, planktonic abundances, ostracod genera from each sample depth, benthic foraminiferal factor scores, and trace element analysis values used in this study. Figure S1 shows depth estimates of the most common taxa present at Bass River in our study. Figure S2 compares global $\delta^{13}C$ values with our study from Bass River. Figures S3–S5 show updated age-depth plots for Sites ACGS#4, Island Beach, and Atlantic City, respectively. Figure S6 compares Bass River BWT/SST with TEX_{86} temperature reconstructions for the Eocene. Please visit https://doi.org/10.1130/GES01652.S1 or access the full-text article on www.gsapubs.org to view the Supplemental Information.

The samples were sieved to acquire the >150 µm fraction, consistent with studies on the margin used for comparison (Browning et al., 1997a; Charletta, 1980; Miller and Katz, 1987; Streeter and Lavery, 1982). The 63–150 µm size fraction was scanned for qualitative analysis. Specimens were picked from the >150 µm size fraction. This approach was employed with the intent to limit the degree of uncertainty due to ambiguity in identifying small specimens including juvenile forms. Although we recognize that some studies prefer picking the >63 µm size fraction in order to minimize underrepresentation of smaller taxa (Thomas, 1990), using the >150 µm size fraction provides information on larger taxa that would otherwise be underrepresented in the >63 µm fraction, where small, hard-to-identify taxa would be highlighted (Katz and Miller, 1996). Study of both the >63 and >150 µm size fractions yield useful data, but we chose the larger size fraction to easily compare with previous studies (e.g., Browning et al., 1997a). Taxonomy from Tjalsma and Lohmann (1983), Jones (1983), Bandy (1949), Enright (1969), Howe (1939), Boersma (1984), van Morkhoven et al. (1986), and Stassen et al. (2015) was used to identify the benthic foraminiferal species in each sample. Species were also compared to type slides and assemblage slides from Browning et al. (1997a) and Charletta (1980). Taxa are well illustrated in these publications.

We calculated benthic foraminiferal numbers (specimens per gram of dry sediment) because they can be related to paleobathymetry especially in fine-grained sediments, although they can be heavily affected by depositional processes in coarse-grained sediments. In general, benthic foraminiferal numbers are inversely related with water depth (Mendes et al., 2004). Percent coarse fraction was calculated using the >63 µm fraction weight versus total sample weight prior to processing. The sand fraction was sieved to separate (1) the fine- and very fine-grained quartz sand and glauconite sand from (2) the medium-grained and coarser quartz sand and glauconite sand. Percent glauconite and shells were visually estimated (Figs. 2, 3).

All benthic foraminifera in each sample split were identified to determine the dominant species, and multivariate analyses were conducted to establish biofacies relationships and trends. The genus *Lenticulina* inhabited the inner shelf to deep sea during the Cenozoic (e.g., Tjalsma and Lohmann, 1983; Katz et al., 2003b). Consequently, *Lenticulina* spp. are not a useful paleodepth indicator and are not included in our analysis of paleobathymetry, although they are found in all of our samples. The benthic foraminiferal data were converted to relative abundances (percentages) and then used to perform Q-mode factor analysis. The data were rotated using the *factoran* function in MATLAB software (version R2013a). Factor analysis is a form of multivariate data reduction that uncovers a simple underlying structure (expressed though variance and covariances) that is presumed to exist within a larger set of observable variables (Davis, 2002). This variance is expressed by placing the variables (in this case, foraminiferal taxa) into unique factors, which we ultimately relate to distinct paleo–water depths. Only factors with eigenvalues >1.0 were considered (Imbrie and Kipp, 1971; Harman, 1976; Guttman, 1954). We chose factor analysis as the primary multivariate method because it yielded useful results in studies we used for comparison (Browning et al., 1997b; Charletta, 1980). Neighbor-joining cluster analysis using Chord similarity index and a final branch root was also performed on taxa occurring at >5% in at least one sample using the PAST 3.13 software (Hammer et al., 2001). Cluster analysis aims to group like variables, independently from other similar variables (Trauth et al., 2010), and is used to further support factor analysis. Diversity indices [Shannon-Wiener heterogeneity index: H; dominance: D; Fisher alpha: $F(\alpha)$; evenness: $e^{H/S}$ (where H is the Shannon-Wiener index and S is the species richness)] were determined to further support assemblage biofacies interpretations. Diversity indices were calculated using initial data sets including all counted benthic foraminiferal specimens. Diversity indices were calculated using the PAST 3.13 software (Hammer et al., 2001).

All planktonic foraminifera in each sample split were counted to determine planktonic foraminiferal percentages relative to total foraminifera. Higher percentages of planktonic foraminifera are generally associated with greater paleodepths (e.g., van der Zwaan et al., 1990).

Stable-Isotope Studies

Both benthic and planktonic foraminifera were analyzed for $\delta^{18}O$ and $\delta^{13}C$ to better understand sea-level and paleoceanographic changes. $\delta^{13}C$ can be measured to help constrain carbon cycle changes (e.g., weathering rates, organic carbon burial, and sources of organic carbon) and used to reconstruct paleocirculation and paleoproductivity. Various carbon reservoirs on Earth have distinctive carbon isotopic signatures, and a change in the storage of one of these reservoirs is reflected in another. Although there is very little fractionation during the precipitation of carbon in carbonate, the role of photosynthesis in organic matter displays a very strong fractionation effect, allowing for the study and interpretation of $\delta^{13}C$ in benthic foraminifera (e.g., Kump and Arthur, 1999; Katz et al., 2010, and references therein).

Foraminiferal $\delta^{18}O_{calcite}$ changes provide a proxy for both temperature and ice volume (e.g., Emiliani, 1955; Shackleton, 1967, 1974; Miller et al., 1991). $\delta^{18}O_{calcite}$ acts as a paleothermometer, with higher values reflecting colder temperatures due to thermodynamic effects (Epstein et al., 1953). It also reflects changes in seawater $\delta^{18}O$ ($\delta^{18}O_{sw}$) due to two effects: (1) growth and decay of isotopically depleted ice sheets that globally change $\delta^{18}O_{sw}$; and (2) local evaporation and precipitation, particularly in the surface ocean. $\delta^{18}O$ analyses were conducted to track both changes upsection (from the lower to upper Eocene) and to determine whether increases in $\delta^{18}O$ occurred across sequence boundaries as predicted by the supposition that these were formed during glacioeustatic falls. Bass River is located in a neritic setting, with the potential of freshwater input (lower $\delta^{18}O_{sw}$), especially during a fall in sea level. However, such effects largely are ameliorated on the middle to outer shelf (water depths >30 m) even in regions with extremely high riverine input (e.g., the modern Amazon; Geyer et al., 1996).

The genus *Alabamina* is the most consistent (present in sequences E3–E10) and well-preserved benthic foraminiferal genus in our section, and is similar

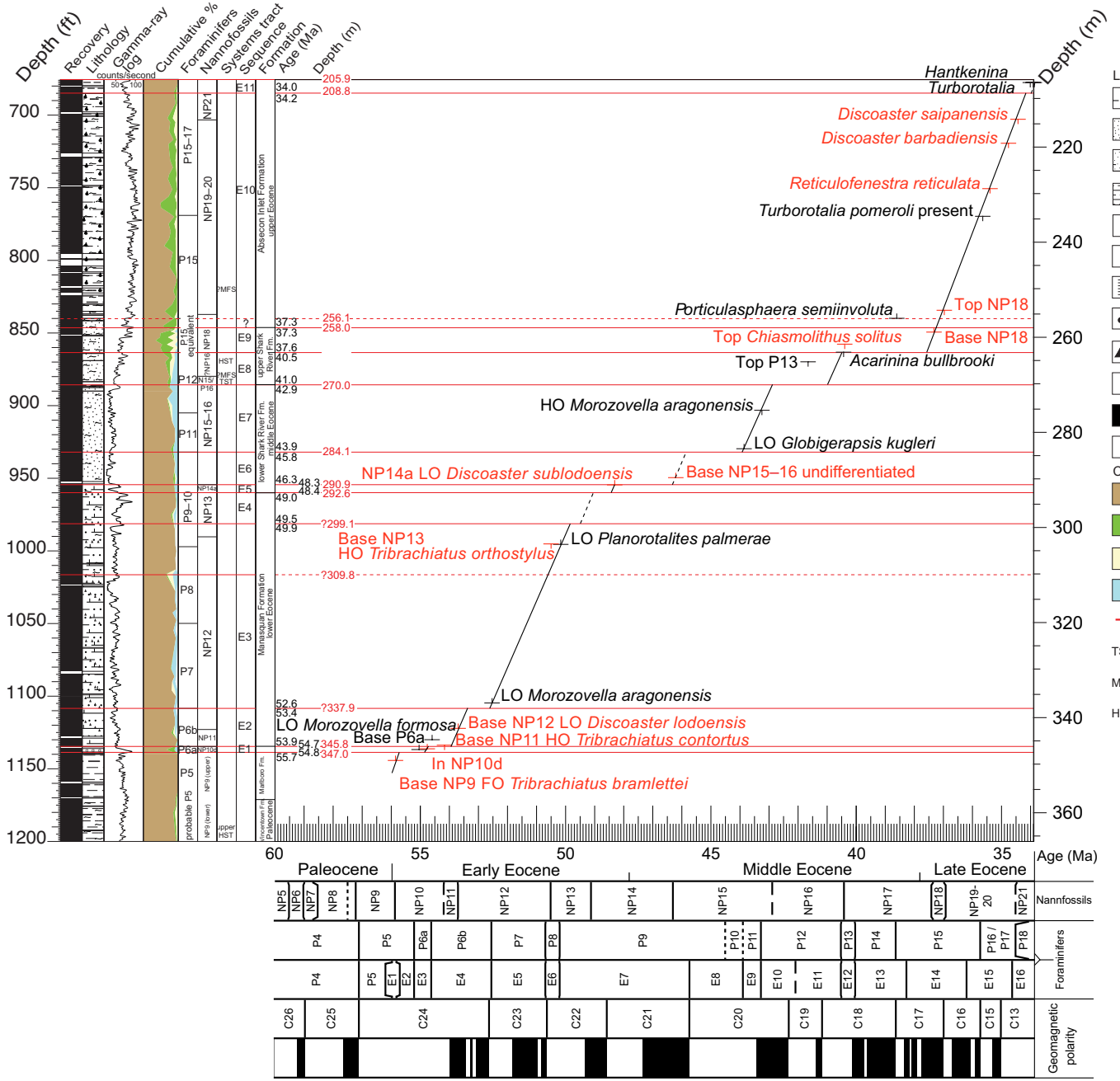

Figure 2. Age versus depth plot for significant biostratigraphic events from the Eocene section of the Bass River borehole, New Jersey coastal plain (USA). Ages of sequence boundaries are shown relative to the Gradstein et al. (2012) time scale. Calcareous nannofossil (red) and planktonic foraminiferal (black) occurrences: LO—lowest occurrence; HO—highest occurrence; FO—first occurrence.. Eocene calcareous nannofossil zones NP9-NP21 are shown. Dashed lines indicate unresolvable contacts (Miller et al., 1998b).

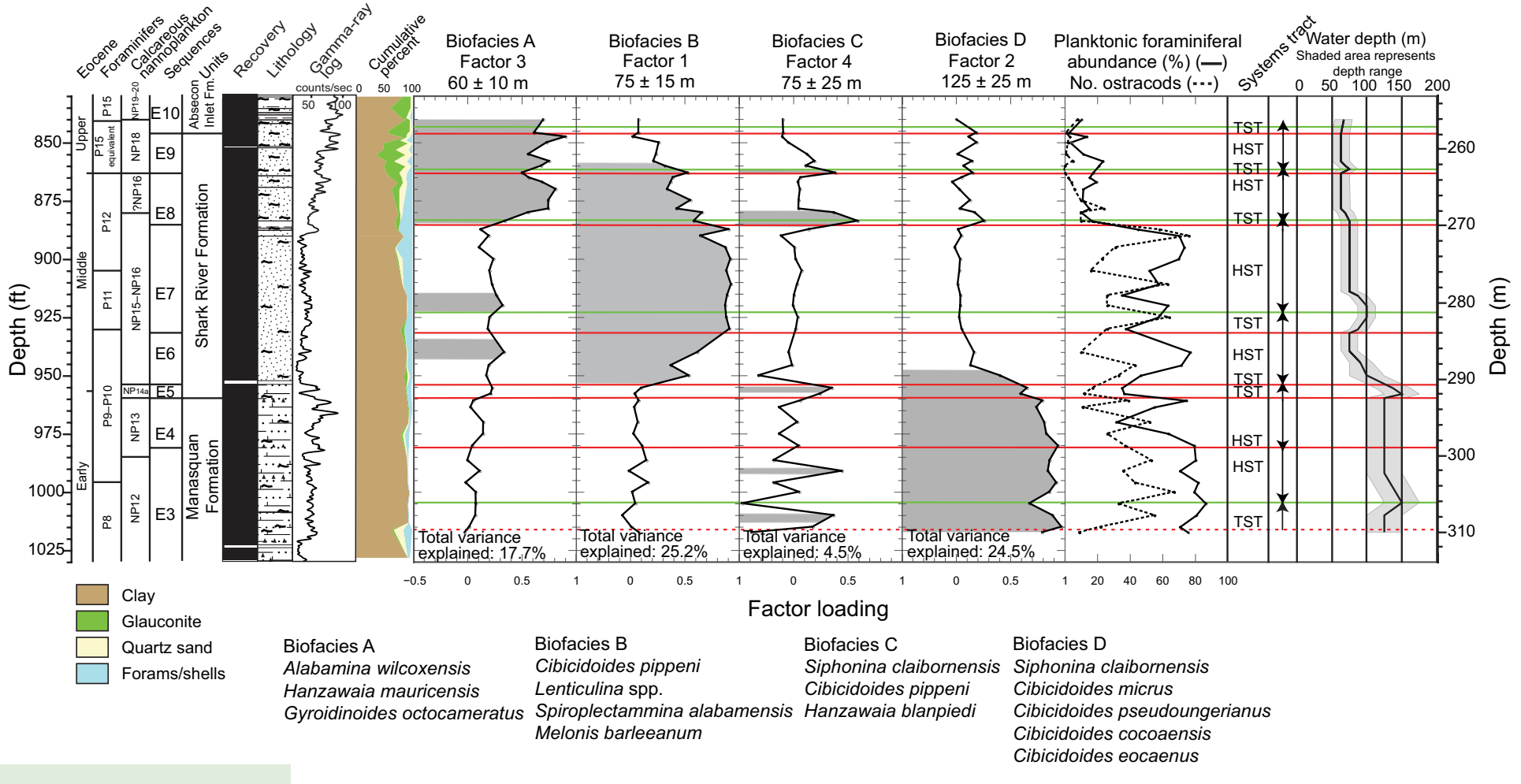

Biofacies A
Alabamina wilcoxensis
Hanzawaia mauricensis
Gyroidinoides octocameratus

Biofacies B
Cibicidoides pippeni
Lenticulina spp.
Spiroplectammina alabamensis
Melonis barleeanum

Biofacies C
Siphonina claibornensis
Cibicidoides pippeni
Hanzawaia blanpiedi

Biofacies D
Siphonina claibornensis
Cibicidoides micrus
Cibicidoides pseudoungerianus
Cibicidoides cocoaensis
Cibicidoides eocaenus

Figure 3. Distribution of lower to middle Eocene benthic foraminiferal factors, planktonic foraminiferal abundances, and number of ostracod genera present at Bass River, New Jersey coastal plain (USA). Shaded areas represent sediments where a particular factor is significant (>0.25 loading). Paleo-water depths (m) for each biofacies and factor are shown. Sequence boundaries (red lines), maximum flooding surfaces (green lines), and the corresponding units and sequences described by Miller et al. (1998b) are shown. Cumulative percent of clay (brown), glauconite (green), quartz sand (tan), and foraminifers/shells (blue) is shown in addition to recovery, lithology, and gamma-ray log from Miller et al. (1988). See Figure 2 for lithology key. Changes in paleowater depth ranges are tracked upsection with arrows pointing in the direction of deepening. TST—transgressive systems tract; HST—highstand systems tract.

in general morphology to the epifaunal genus *Cibicidoides,* a taxon generally favored in stable-isotopic studies (e.g., Katz et al., 2010). To provide the most comprehensive isotopic analysis of the section, two species of *Alabamina* (*A. wilcoxensis* and *A.* aff. *dissonata*) and four species of *Cibicidoides* (*C. cocoaensis*, *C. pippeni, C. eocaenus, C. pseudoungerianus*) were analyzed. Note that the last occurrence of *A.* aff. *dissonata* is in the sample at corehole depths 288.9 m (945.7 ft), and 285.6 m (936.9 ft) marks the first occurrence of *A. wilcoxensis*. Two genera of planktonic foraminifera (surface-dwelling *Acarinina* and thermocline-dwelling *Subbotina*) were also analyzed across the E4-E5 and E5-E6 sequence boundaries. These sequence boundaries were chosen for analysis because the benthic foraminiferal $\delta^{18}O$ increased significantly at these sequence boundaries. Comparisons show species offsets that result from microhabitat preferences, such as infaunal versus epifaunal benthics, surface- versus thermocline-dwelling planktonics, and vital effects (variation in metabolic processes) (e.g., Rohling and Cooke, 1999; Katz et al., 2003c, 2010). Infaunal benthic foraminifera live within the sediments and record pore-water chemistry, and are therefore helpful indicators of productivity. During a period of high productivity in the surface waters, an increase in organic matter is delivered to the sediments, which release ^{12}C when oxidized and drive down $\delta^{13}C$ in the pore waters. Epifaunal benthic foraminifera live at or near the sediment-water interface, and therefore more closely reflect seawater $\delta^{13}C$ values and are good water-mass tracers (e.g., Mackensen et al., 2000; Shackleton et al., 2000).

Specimens of these species were picked from each sample and sonicated in distilled water to remove clays. Only well-preserved glassy specimens were analyzed. Approximately four to seven specimens of each benthic foraminiferal taxon were chosen from each sample for analysis. Multiple analyses were conducted for the same sample to compare the genus *Alabamina* with *Cibicidoides*.

Samples were analyzed at the Stable Isotope Laboratory in the Department of Earth and Planetary Sciences at Rutgers University (Piscataway, New Jersey) using a Micromass Optima mass spectrometer. Foraminifera were reacted with phosphoric acid at 90 °C for 15 min. Stable-isotope values are reported versus Vienna Peedee belemnite (V-PDB) by analyzing standard NBS-19 and an internal laboratory standard during each automated run. The internal laboratory standard is calibrated against NBS-19, with an offset of ±0.04‰ and ±0.10‰ for $\delta^{18}O$ and $\delta^{13}C$, respectively. Results are reported relative to the V-PDB standard. The laboratory standard error (1σ) is ±0.08‰ for $\delta^{18}O$, and ±0.05‰ for $\delta^{13}C$.

Magnesium/Calcium Studies

Two species of benthic foraminifera (*C. pippeni* and *C. eocaenus*) and two genera of planktonic foraminifera (*Acarinina* and *Subbotina*) were chosen for Mg/Ca analysis based on their preservation and distribution. On average, 19 specimens of each benthic species and 42 of each planktonic genus were selected from each sample for analysis. Individual specimens of these species were picked from each sample, sonicated in distilled water to remove clays, weighed, and crushed between glass plates. The crushed foraminiferal tests were chemically cleaned following the Cd-cleaning protocol modified by Rosenthal et al. (1997). Trace element analyses (Sr/Ca, B/Ca, Mg/Ca, Mn/Ca, Al/Ca, and Fe/Ca) were measured at the Department of Marine and Coastal Sciences at Rutgers University (New Brunswick, New Jersey) on a Thermo Finnigan Element XR sector field–inductively coupled plasma–mass spectrometer (SF-ICP-MS) following the method of Rosenthal et al. (1999).

Trace element values are noted to ensure that the analyzed specimens do not indicate the likelihood of contamination (Table S1 [footnote 1]). To calculate the Mg/Ca temperature, we used a corrected exponential calibration following Evans and Müller (2012), where modern seawater is 5.2 mmol/mol, Eocene seawater is 2.0 mmol/mol (see summary in Cramer et al., 2011), and *H* (which is a constant calibrated for a specific group or species) = 0.41; the constants A (0.109) and B (0.867) for benthic foraminifera are from Lear et al. (2002), and A (0.09) and B (0.38) for planktonic foraminifera are from Anand et al. (2003); T is temperature, t = 0 is present, and t = t is some point in the past.

$$\mathrm{Mg/Ca_{test}} = \frac{\mathrm{Mg/Ca_{sw}^{t=t^H}}}{\mathrm{Mg/Ca_{sw}^{t=0^H}}}\ B\ 10^{\mathrm{AT}}. \quad (1)$$

Estimates of $\delta^{18}O_{sw}$, a measure of ice volume, were calculated by substituting the Mg/Ca temperature and $\delta^{18}O_{test}$ into the modified paleotemperature equation of Cramer et al. (2011), modified after Lynch-Stieglitz et al. (1999):

$$T(^{\circ}\mathrm{C}) = 16.1 - 4.76\ \left(\delta^{18}O_{test} - \left(\delta^{18}O_{sw} - 0.27\right)\right). \quad (2)$$

Although the absolute temperature depends on the Mg/Ca_{sw} composition correction applied and species-specific coefficients, the overall magnitude of change does not (Babila et al., 2016). The limited availability of well-preserved specimens across multiple sequence boundaries made it difficult to better constrain temperature and $\delta^{18}O_{sw}$ reconstructions for a single species. As a result, benthic foraminiferal $\delta^{18}O_{sw}$ reconstructions across the E2-E3 sequence boundary were calculated using *C. pseudoungerianus* Mg/Ca and $\delta^{18}O$ values; across the E4-E5 sequence boundary using *C. eocaenus* Mg/Ca and $\delta^{18}O$ values; and across the E5-E6 and E6-E7 sequence boundaries using *C. pippeni* Mg/Ca and $\delta^{18}O$ values. Planktonic foraminiferal $\delta^{18}O_{sw}$ reconstructions from E4–E6 were calculated using surface-dwelling *Acarinina* spp. Mg/Ca and $\delta^{18}O$ values and thermocline-dwelling *Subbotina* spp. Mg/Ca and $\delta^{18}O$ values. When multiple species are used, an interspecies isotopic correction factor is essential to account for vital effects (e.g., Katz et al., 2003c). Specimens of *C. pippeni* and *C. eocaenus* from the same sample depths within E5 allowed us to calculate a species correction and present a continuous single-species temperature and $\delta^{18}O_{sw}$ record for *C. pippeni* from E4–E6. In order to evaluate the temperature component of $\delta^{18}O_{calcite,}$ planktonic and benthic foraminifera were analyzed from sequences E4–E7 with a focus on the E4-E5 and E5-E6 sequence boundaries.

Ostracod Studies

All ostracods from each benthic foraminiferal split were picked for analysis and interpretation. Taxonomy from Swain (1951), Krutak (1961), Hazel (1968), and Deck (1985) was used to identify a total of 17 ostracod genera at Bass River. The number of valves was counted to determine the abundance of genera and the number of genera per sample for each sample. Four diversity indices—Shannon-Wiener index (H), dominance (D), Fisher alpha [$F(\alpha)$], and evenness ($e^{H/S}$)—were calculated using initial data sets including all counted ostracod specimens. The number of whole carapaces (two valves) in each sample was also noted to calculate percent valves.

Sequence Boundaries

Descriptions of sedimentary textures, colors, fossil content, and lithostratigraphic units (New Jersey Geological Survey, 1990) are presented in Miller et al. (1998b). Unconformities were distinguished by sharp gamma-ray peaks, bioturbation, reworking, changes in major lithofacies, and changes in lithologic stacking patterns (Miller et al., 1998b). In this study, we build on the sequence stratigraphic framework of Browning et al. (1997b) and Olsson and Wise (1987), who identified unconformities in other coastal plain coreholes based on abrupt changes in lithology and benthic foraminiferal biofacies and gaps in planktonic and calcareous nannoplankton zones (Browning et al., 1997b). We present an age-depth diagram for significant biostratigraphic events from the Eocene section of the Bass River corehole, and this is our basis for our age model (Fig. 2) and temporal correlations). We constructed our chronology by integrating calcareous nannofossil and planktonic foraminiferal biostratigraphy on an age-depth diagram. These relatively deep-water sections had abundant plankton, although not all primary markers were present. The age-depth diagram presented here uses the data in the Bass River site report with the ages of biostratigraphic events updated to the Gradstein et al. (2012) time scale. Sedimentation rates were estimated on the age-depth plots (Bass River, Fig. 2; ACGS#4, Island Beach, and Atlantic City, Figs. S3–S5 [footnote 1]) as visual best fits to the biostratigraphic datum levels. In cases where only one reliable datum level was available for a sequence (e.g., E8 at Island Beach or E10 at ACGS#4), an average sedimentation rate of 40 m/m.y. found in this and previous studies (e.g., Browning et al., 1997a) was fit to the data within the constraints of superposition. Age errors are ±0.5–1 m.y. with this approach (Browning et al., 1996). Samples are tied to the age model based on interpolation of the depth of the sample relative to the ages of the upper and lower sequence boundaries. Lithology, gamma-ray log, cumulative coarse fraction percent, and biostratigraphic markers are also plotted. Deepening-upward successions are interpreted as TSTs and exhibit fining-upward successions, whereas shallowing-upward successions are indicative of HSTs and show coarsening upward. LSTs were not identified, consistent with previous work. Gamma-ray logs for coastal plain sediments record largely a trivariate response, with lower values for quartz-rich sediments, higher values for muds, and even higher values for sediments containing glauconite sand (Lanci et al., 2002).

RESULTS

Factor Analysis

Forty-three (43) samples were examined from the lower Eocene to lower upper Eocene, and a total of 116 species were identified from ~10,017 benthic foraminiferal specimens at Bass River (Table S1 [footnote 1]). Benthic foraminiferal factor analysis delineated four factors that explain 72% of the faunal variation (Figs. 3–7; Table S1 [footnote 1]). We use the resulting four biofacies to interpret paleodepths on the continental shelf. Depth ranges for individual species have been previously estimated (Browning et al., 1997a; Olsson and Wise, 1987). We provide a compilation of depth ranges for the most common taxa in our studied section (Fig. S1 [footnote 1]). We compare our results from factor analysis to the biofacies and corresponding depths described by Browning et al. (1997a) for three New Jersey coreholes. The biofacies, and the factors that explain them, are discussed below from shallowest (biofacies A) to deepest (biofacies D). Within each factor we show species with the highest three loadings (or more if *Lenticulina* spp. and/or more environmentally significant species are present). Eocene sediments at Bass River are fossiliferous enough to contain well-preserved biostratigraphic marker taxa, allowing for planktonic foraminiferal and calcareous nannoplankton zonation (Miller et al., 1998b). Species abundance plots for the most common taxa in our studied interval are shown in Figure 8.

Although not expressed in the factor plots, *Globobulimina ovata* has a low relative abundance throughout the section, except at corehole depths 257.8 m and 304.8 m (845.9 ft and 1000 ft), where it is has the third- and second-highest percentage respectively. This may indicate low-oxygen conditions (Jorissen et al., 1998).

Biofacies A

Factor 3 (biofacies A) describes 17.7% of the total faunal variation. The taxa with the highest scores are *Alabamina wilcoxensis* (score = 5.98), *Hanzawaia mauricensis* (score = 3.78), *Gyroidinoides octocameratus* (score = 3.74), *Hanzawaia blanpiedi* (score = 3.29), *Cibicidoides cocoaensis* (score = 3.12), *Cibicidoides praemundulus* (score = 2.09), and *Uvigerina* spp. (score = 0.98) (Figs. 3 and 4). The high negative score for *Spiroplectammina alabamensis* (–2.15) indicates that this species is inversely correlated with biofacies A. This biofacies at Bass River is similar to biofacies A from other New Jersey coastal plain sites (Island Beach, Atlantic City, and ACGS#4) of Browning et al. (1997a), with paleodepths of 60 ± 10 m, and is associated with high abundances of glauconite and siliciclastic sediment. Low average planktonic foraminiferal abundance

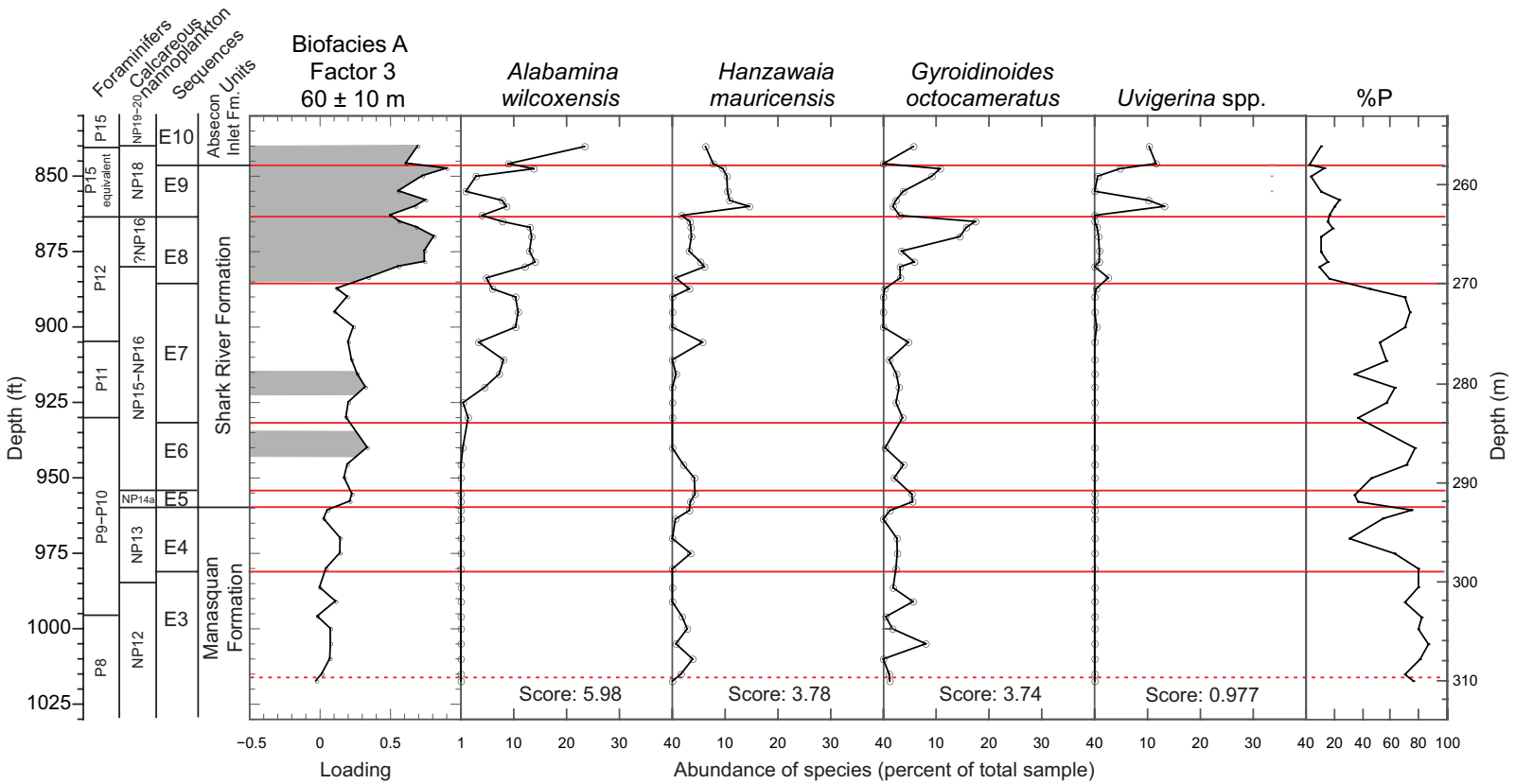

Figure 4. Biofacies A (factor 3 and associated paleo-water depths). Distribution of species with high loadings are shown (percent of total sample). Total variance explained: 17.7%. Red lines represent sequence boundaries; dashed line within sequence E3 indicates an unresolvable contact and may represent a sequence boundary (Miller et al., 1998b). %P—planktonic foraminiferal abundance. Scores show how strongly an individual species relates to the factor.

(13%), ostracod diversity [*H*= 1], and ostracods per sample (6) correspond with this biofacies. The highest loadings for biofacies A are in the 13 samples from the upper Shark River Formation in sequences E8–E10. Biofacies A essentially represents the glauconitic and sandy upper Shark River assemblage.

Biofacies B

Factor 1 (biofacies B) describes 25.2% of the total faunal variation. The taxa with the highest scores are *Cibicidoides pippeni* (score = 8.33), *Lenticulina* spp. (score = 4.50), *Spiroplectammina alabamensis* (score = 3.20), and *Melonis barleeanum* (score = 2.01) (Figs. 3 and 5). This biofacies dominates the lower Shark River Formation (sequences E6 and E7) and is found at the base of sequence E8 (upper Shark River Formation), and describes 15 samples. Biofacies B essentially represents the shelly and calcareous lower Shark River assemblage. Biofacies B is similar to biofacies B in Browning et al. (1997a), indicating paleodepths of 75 ± 15 m. The average planktonic foraminiferal abundance for samples in this biofacies is 58%, indicating deeper-water deposition than in biofacies A.

Biofacies C

Factor 4 (biofacies C) describes 4.5% of the total faunal variation and is dominated by *Siphonina claibornensis* (score = 8.07), *Cibicidoides pippeni* (score = 3.21), and *Hanzawaia blanpiedi* (score = 1.36). Though the percent explained is low, this is the same biofacies identified across the shelf by Browning et al. (1997a, their bifoacies D). Based on depth ranges for these taxa, we estimate paleodepths of 75 ± 25 m (Figs. 3 and 6), which helps characterize six samples. Biofacies C is found at the base of sequences E8 and E9,

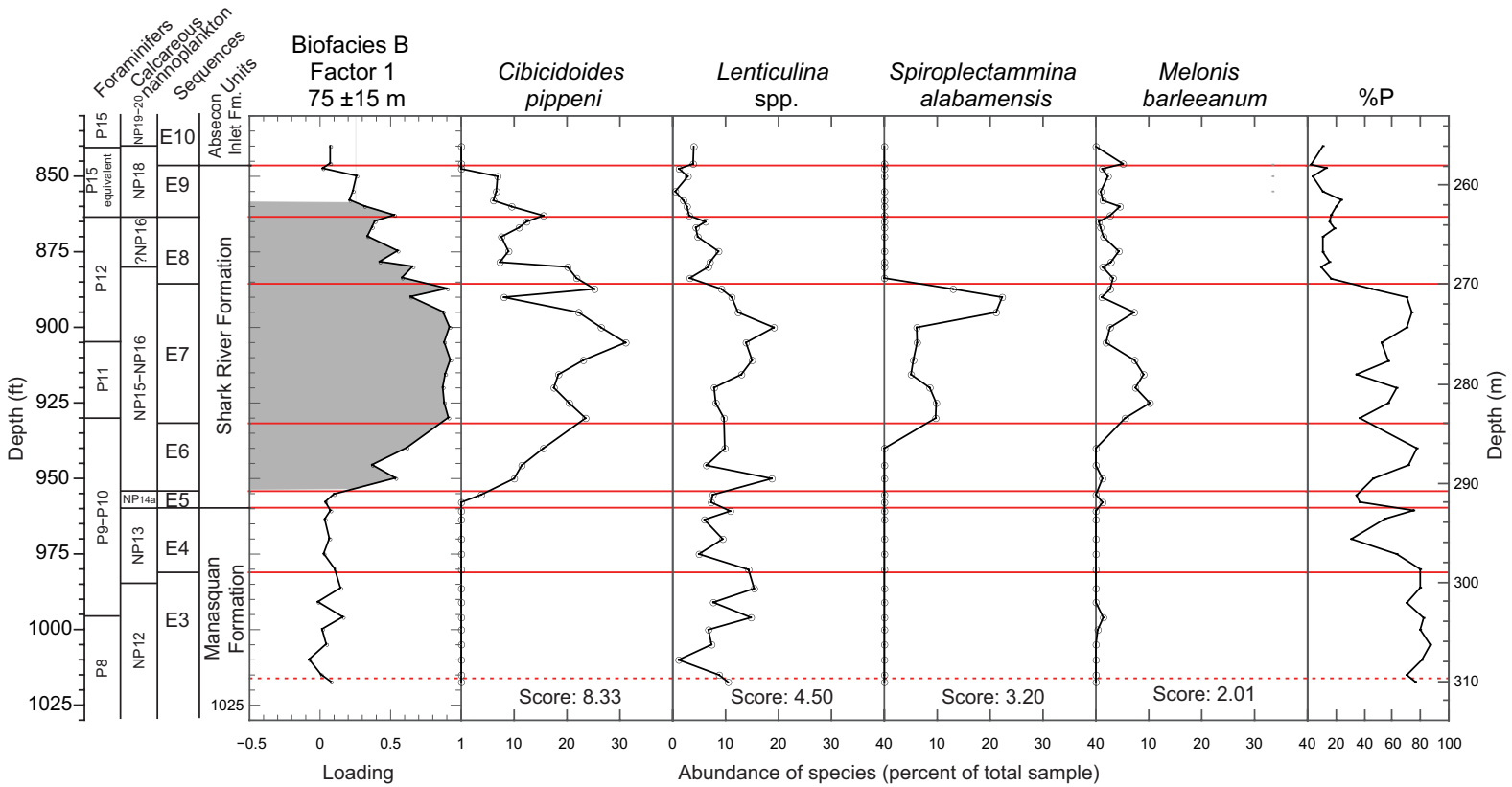

Figure 5. Biofacies B (factor 1 and associated paleo-water depths). Distribution of species with high loadings are shown (percent of total sample). Total variance explained: 25.2%. Red lines represent sequence boundaries; dashed line within sequence E3 indicates an unresolvable contact and may represent a sequence boundary (Miller et al., 1998b). %P—planktonic foraminiferal abundance. Scores show how strongly an individual species relates to the factor.

marking a deepening-upward trend that is indicative of the TSTs. Biofacies C allows us to clearly define the basal TSTs within sequences E8 and E9. Similar peaks are found in sequences E3 and E5, but *C. pippeni* is absent and is not considered significant. The average planktonic foraminiferal abundance found at the base of sequences E8 and E9 is 13% and 19%, respectively. The combination of biofacies C with biofacies B and D provides further refinement within these sequences.

Biofacies D

Factor 2 (biofacies D) describes 24.5% of the total faunal variation, and biofacies D characterizes 15 samples. The taxa with the highest scores are *Siphonina claibornensis* (score = 6.52), *Cibicidoides micrus* (score = 4.83), and *Cibicidoides pseudoungerianus* (score = 4.73). Other important species in this biofacies are *Cibicidoides cocoaensis* (score = 2.28), *Cibicidoides eocaenus* (score = 1.66), *Eponides jacksonensis* (score = 1.05), and *Alabamina* aff. *dissonata* (score = 0.62) (Figs. 3 and 7). *Cibicidoides micrus* is similar to, and may be the same species as, *Anomalinoides acuta* (Browning et al., 1997a). *Cibicidoides eocaenus* was primarily a bathyal species (Browning et al., 1997a), and the occurrence of this species gives this biofacies the greatest paleowater depths found within our section (sequences E3–E5) at the Bass River site. The switch from *A. wilcoxensis* to *A.* aff. *dissonata* (Tjalsma and Lohmann, 1983) supports the interpretation of deeper water depths. This biofacies is similar to biofacies D in Browning et al. (1997a), which is found in clay-rich sediments, with paleodepths of 125 ± 25 m. The average planktonic foraminiferal abundance in samples characterized by this biofacies is 67%, with some samples reaching as high as 82%, supporting the greater water depth interpretation.

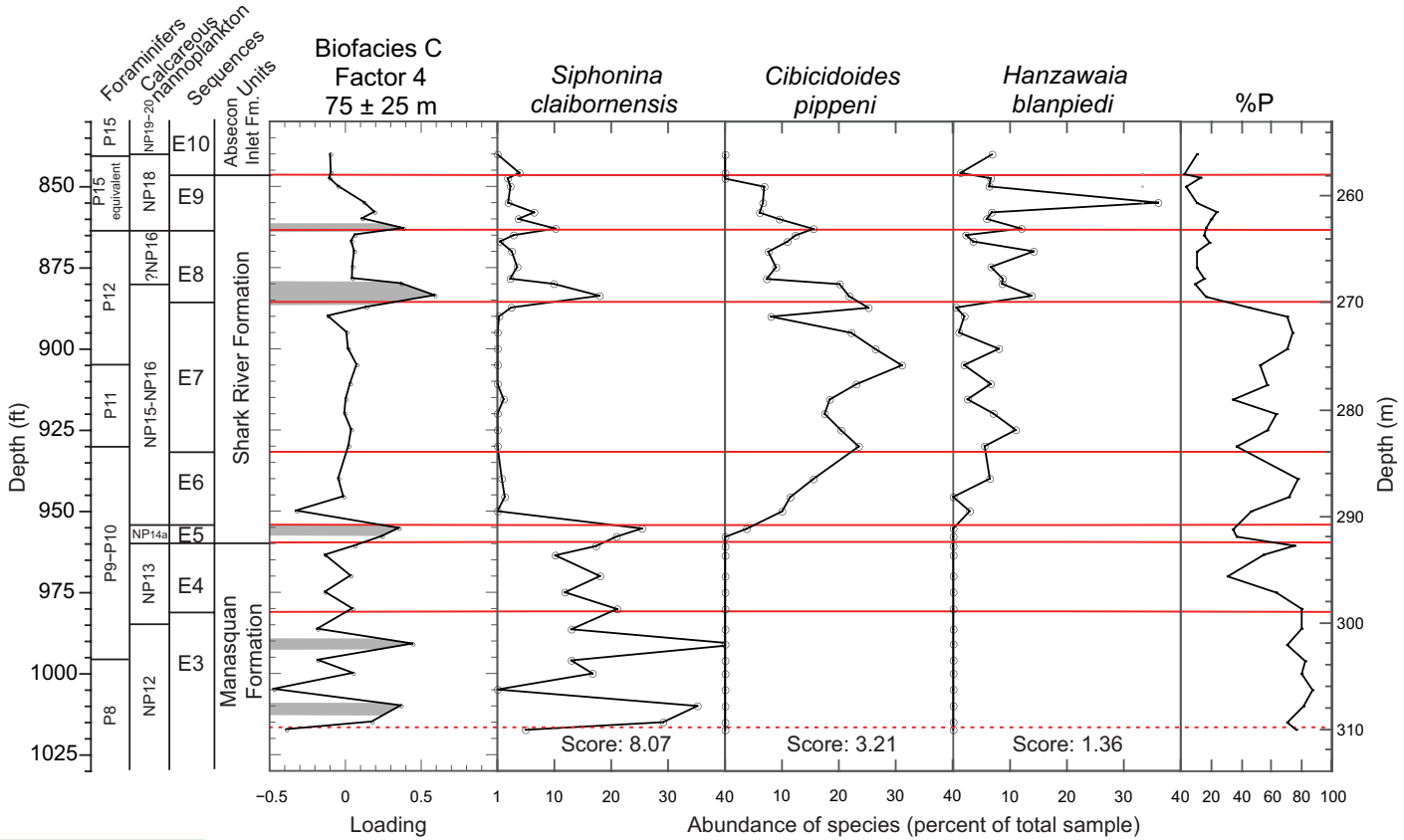

Figure 6. Biofacies C (factor 4 and associated paleo-water depths). Distribution of species with high loadings are shown (percent of total sample). Total variance explained: 4.5%. Red lines represent sequence boundaries; dashed line within sequence E3 indicates an unresolvable contact and may represent a sequence boundary (Miller et al., 1998b). %P—planktonic foraminiferal abundance. Scores show how strongly an individual species relates to the factor.

Biofacies D is found in the lower Eocene of sequences E3–E5 and is essentially the Manasquan Formation assemblage, which transitions into biofacies B of the lower Shark River Formation.

Diversity Indices, Foraminiferal Numbers, and Grain Size

Diversity indices were calculated using initial data sets including all counted benthic specimens from 42 samples at Bass River (Fig. 9). Heterogeneity [Shannon-Wiener *H*] ranges from 2.0 to 3.2, dominance (*D*) ranges from 0.1 to 0.2, Fisher $F(\alpha)$ ranges from 3.5 to 12, and evenness ($e^{H/S}$) ranges from 0.4 to 0.7. Shannon-Wiener *H* and $F(\alpha)$ values tend to increase at the bases of sequences, followed by a decrease upsection. Highest diversity is observed within sequence E8. Dominance (*D*) remains relatively uniform throughout the studied interval, with prominent increases occurring near the tops of sequences E3, E5, E7, E8, and E9. Evenness ($e^{H/S}$), which is the opposite of dominance, remains relatively stable in our section, with decreases occurring in the upper sections of sequences E3, E7, and E8. Diversity indices can be used to assess environmental stability; communities are considered stable if the Shannon-Wiener *H* index remains between 2.5 and 3.5, in transition between 1.5 and 2.5, and stressed below 1.5 (Magurran, 1988; Patterson and Kumar, 2000; Roe and Patterson, 2014). The majority of samples (79%) remain above stable levels [i.e., Shannon-Wiener $H>2.5$], with transition-level values occurring at the base of sequence E3 and near the tops of sequences E3, E7, and E9.

Benthic foraminiferal numbers (specimens per gram) generally are constant through sequences E3 and E4. These numbers increase gradually to a maximum in sequence E8, which coincides with the highest *H* values, and then decline into sequence E10 (Fig. 9).

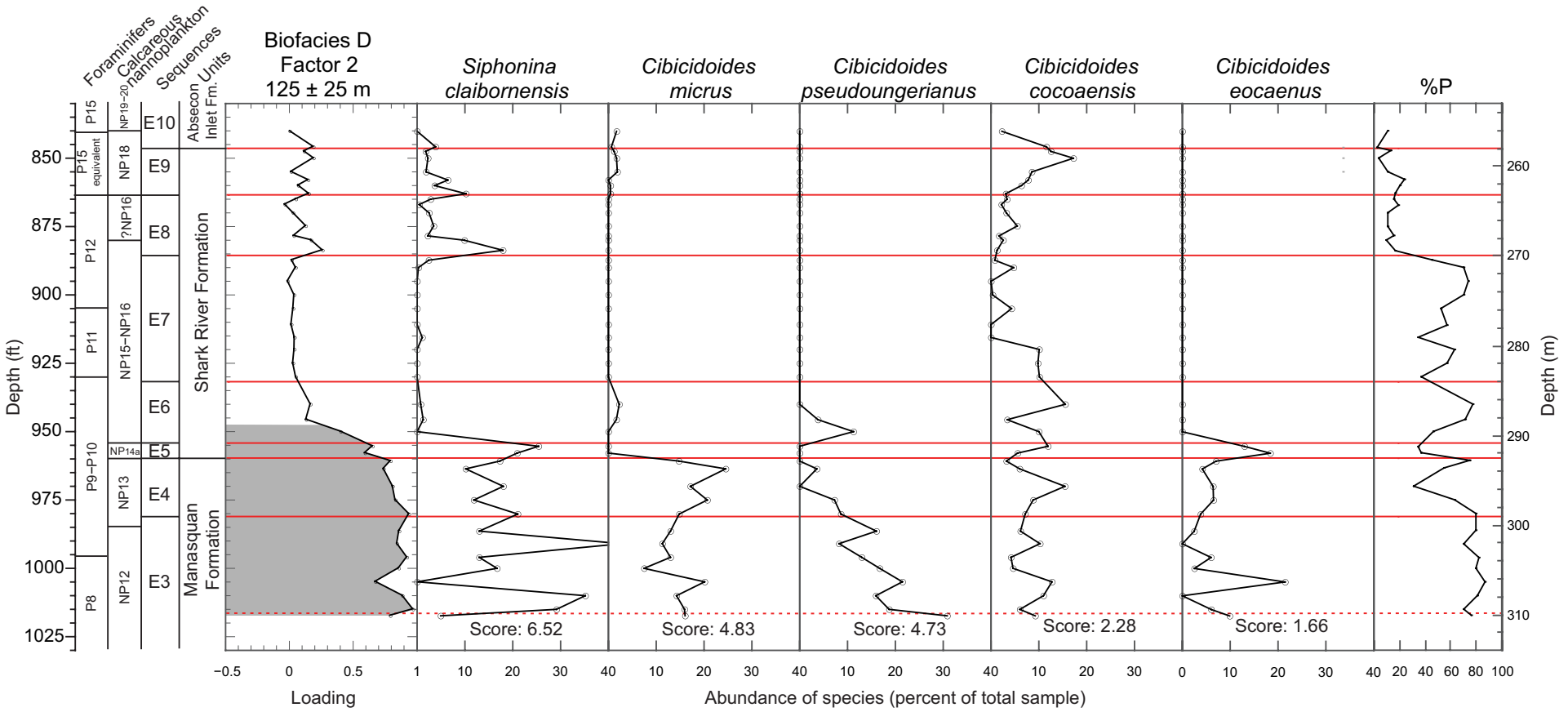

Figure 7. Biofacies D (factor 2 and associated paleo-water depths). Distribution of species with high loadings are shown (percent of total sample). Total variance explained: 24.5%. Red lines represent sequence boundaries; dashed line within sequence E3 indicates an unresolvable contact and may represent a sequence boundary (Miller et al., 1998b). %P—planktonic foraminferal abundance. Scores show how strongly an individual species relates to the factor.

The coarse fraction (>63 µm) generally consists primarily of quartz or glauconite sands, where glauconite in TSTs is in situ and in HSTs is reworked based on its covariance with quartz sand (Miller et al., 2004). The percent coarse fraction is low (average 11%) throughout sequences E3–E7 (Fig. 9), increases in the upper section of sequence E7, and reaches a maximum of 64% in sequence E9 (where it consists of an admixture of quartz and reworked glauconite sand; Figs. 2, 3), followed by a decrease to 12% in sequence E10. The increase in percent coarse fraction throughout our studied interval of ~20 m.y. indicates an overall long-term shallowing trend. Within individual sequences (specifically E3, E4, E5, E7, E8, E9), we observe a coarsening-upward trend (Figs. 2, 3), indicative of shallowing upsection.

Cluster Analysis

Cluster analysis was performed on the relative abundances of the 31 most common benthic foraminiferal taxa (>5% in at least one sample) (Fig. 10) and supports factor analysis interpretations. Clusters are based on a consistent level of similarity. The boxes in Figure 10 show the clusters, which are related to the biofacies determined by factor analysis. The first three factors (biofacies B, biofacies D, and biofacies A) are distinctly clustered, whereas factor 4 (biofacies C) is less definite. This clustering is consistent with the fact that the first three factors account for ~68% of the total variance and each is

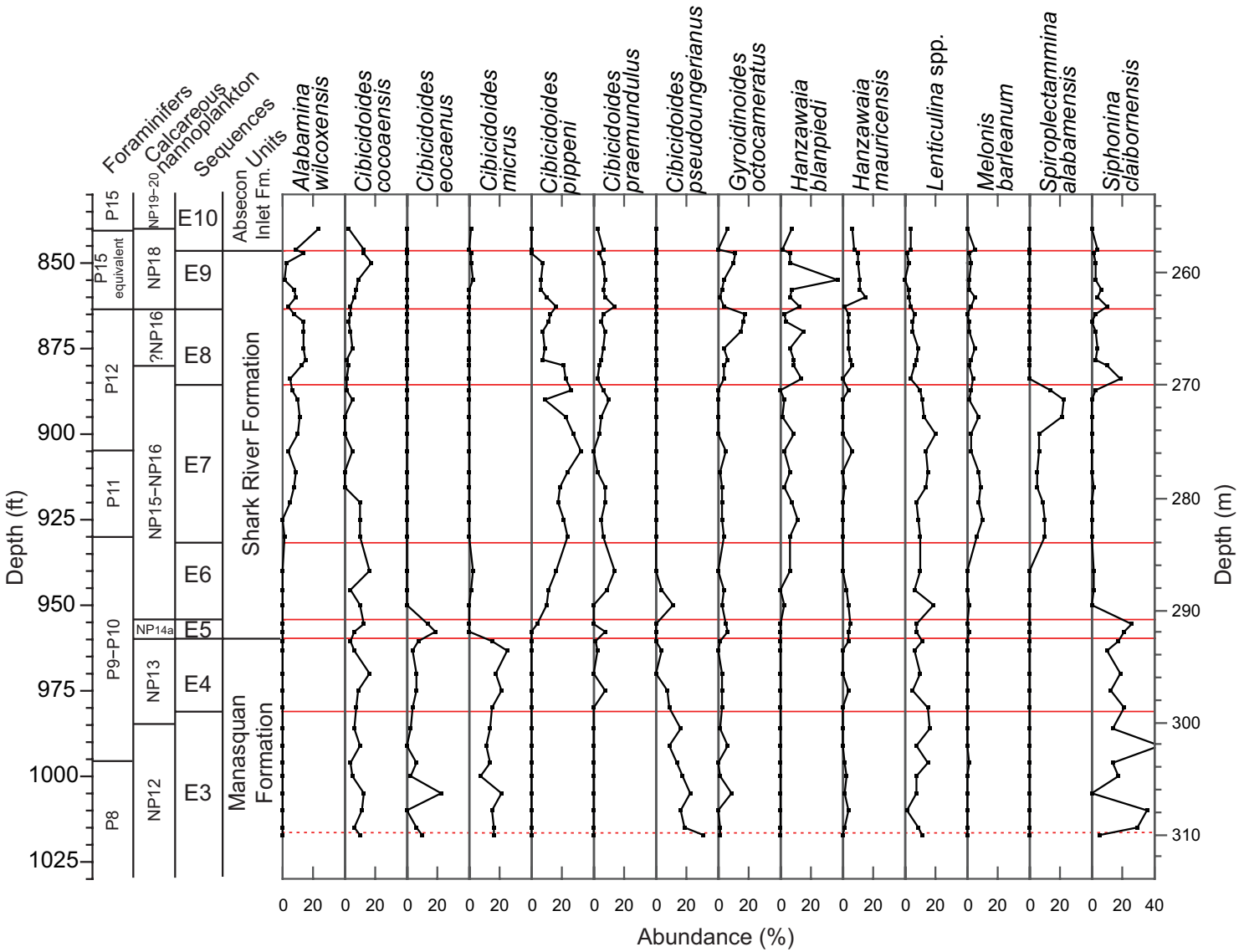

Figure 8. Abundance plot of the most common species in the lower to upper Eocene section at Bass River, New Jersey coastal plain (USA).

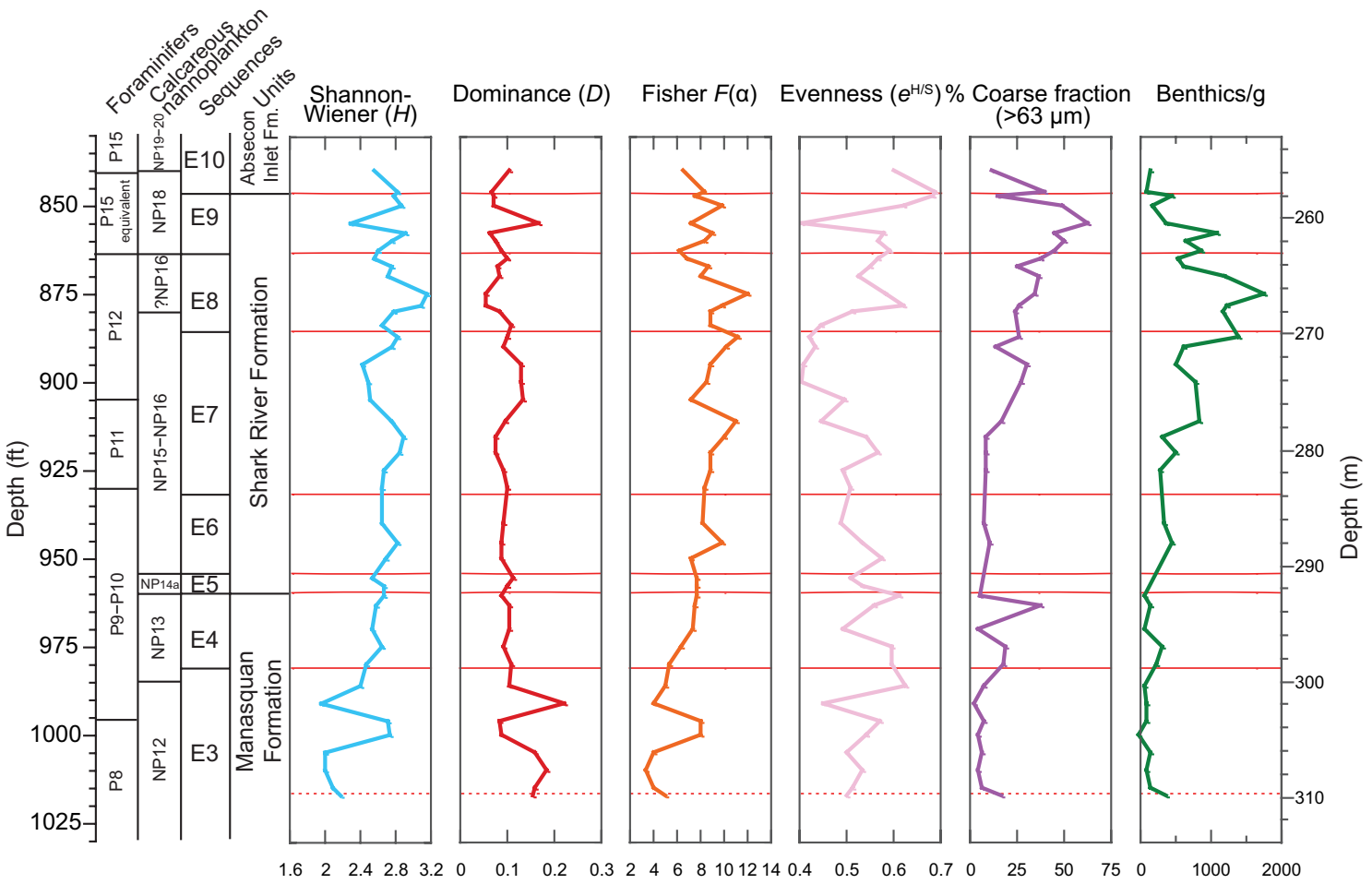

Figure 9. Plot of benthic foraminiferal diversity indices [Shannon-Wiener heterogeneity index: *H*; dominance: *D*; Fisher alpha: *F*(α); evenness: $e^{H/S}$ (where H is the Shannon-Wiener index and S is the species richness), percent coarse fraction (>63 μm), and benthic foraminiferal numbers per gram present at Bass River, New Jersey coastal plain (USA).

characterized by three to five species with high scores. Factor 4, on the other hand, is characterized by only one high-scoring species and contains species that also appear in the first two factors.

Ostracods

Seventeen ostracod genera were identified from the 1093 specimens at Bass River (Table S1 [footnote 1]). The number of ostracods within each sample tends to track planktonic foraminiferal abundance (Fig. 3). The largest number of total preserved ostracods in the sample and highest ostracod generic diversity indices (Fig. 11) occur through sequences E3–E8, with a dramatic drop in heterogeneity [Shannon-Weiner *H*], diversity [Fisher *F*(α)], and the number of observed genera occurring in the upper section of sequence E8 and continuing through E10. The average number of genera present in sequences E3–E7 is ~8, and in sequences E8–E10 is ~3. Conversely, dominance (*D*) remains low within sequences E3–E8 and increases going into sequences E8–E10. Greatest ostracod diversity is found at corehole depths 304.8, 289.6, 281.9, and 270.4 m (1000, 950,

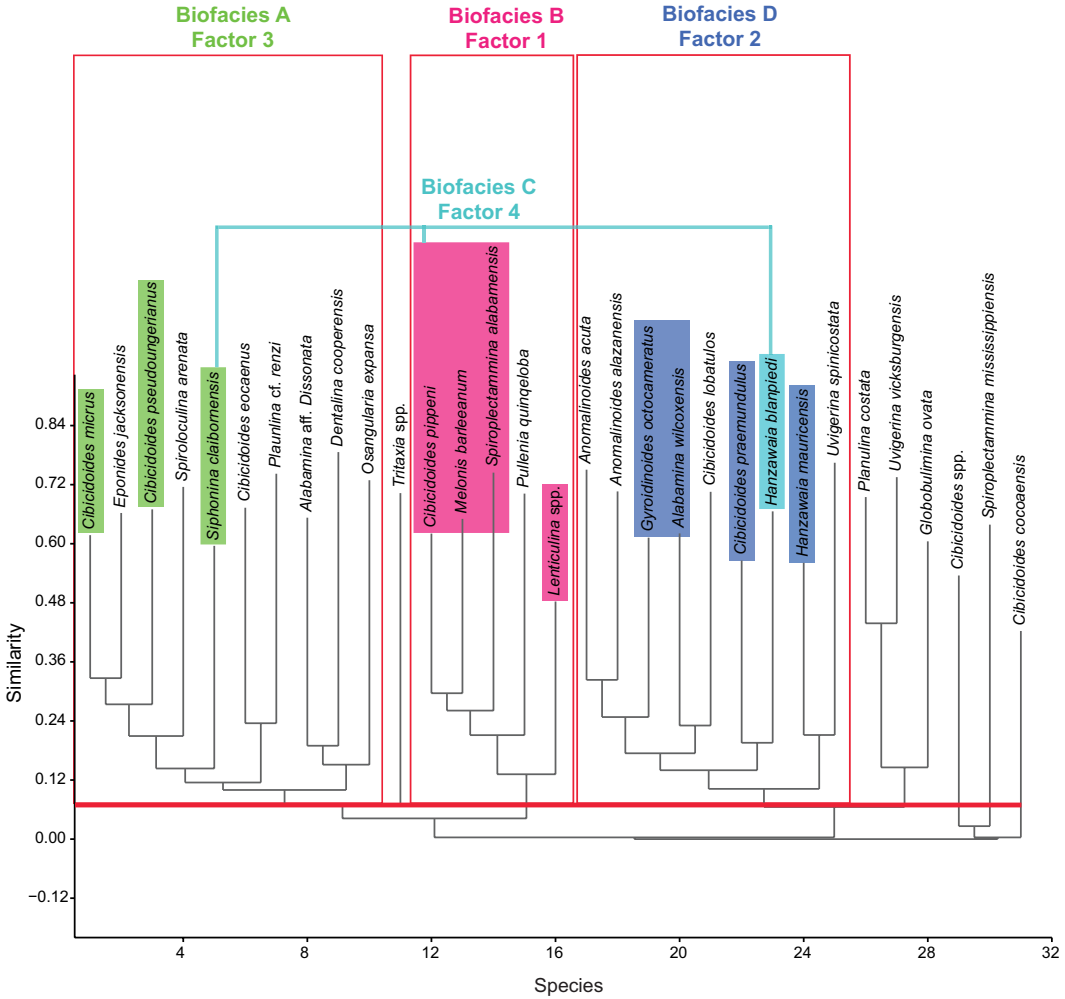

Figure 10. Neighbor-joining cluster analysis using a Chord similarity index and final branch root performed on the relative abundance of the 31 most common taxa (>5% in at least one sample). Clusters are based on a consistent level of similarity (heavy red line). Red boxes show related clusters and the corresponding biofacies and factors that explain them. The highest loading species for each biofacies are shaded accordingly.

925, and 887 ft), coinciding with peaks in number of preserved ostracods. We also find the maximum number of preserved whole carapaces (also known as lowest percent valves) at these sample depths. The percent valves dramatically increases to 100% in the upper section of sequence E8 and continues through E10. At this depth, *Eucythere* (typical of deeper water in the outer shelf; Whatley, 1988) disappears completely from our study upsection. We also observe a switch from delicately ornamented genera to more heavily calcified and robust ostracods in the upper section of sequenced E8. Furthermore, spinose ostracods (e.g., *Acanthocythereis* and *Actinocythereis*) disappear and are replaced by smooth-walled genera in sequences E9 and E10 (Table S1 [footnote 1]).

Taphonomy

The taphonomic condition of paleo-continental New Jersey sediments needs to be taken under consideration in order to make accurate paleoenvironmental interpretations (Stassen et al., 2015). Despite potential taphonomic effects (discussed below), the distinctive and discrete faunal patterns noted within and between sequences (Fig. 3) and among studies (e.g., the similar changes noted by Browning et al., 1997a, 1997b) argue for minimal overprint of the original biocenosis. Although foraminifera are generally well preserved at Bass River, benthic foraminiferal preservation does vary through the studied section, from poor to

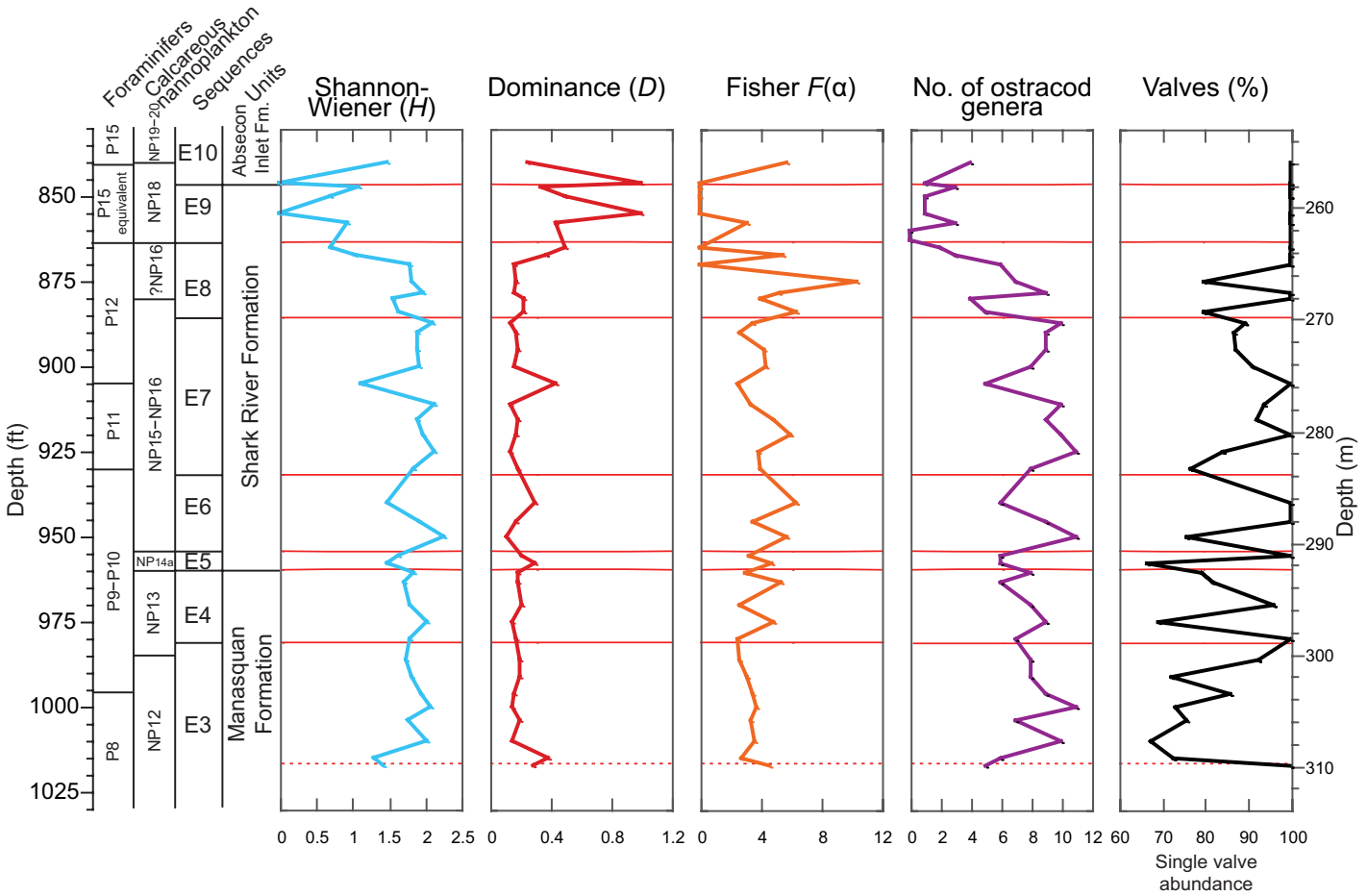

Figure 11. Plot of ostracod diversity indices [Shannon-Wiener heterogeneity index: *H*; dominance: *D*; Fisher alpha: *F*(α)], number of ostracod genera, and percent valves (single valve abundance) present at Bass River, New Jersey coastal plain (USA).

excellent, indicating variable taphonomic effects in different lithologies. In general, we find that foraminifera are less translucent in the sandy sediments than in the clays. Near the condensed sections associated with the MFS, specifically at corehole depths 306.2, 269.1, and 263.0 m (1005, 883, and 863 ft), foraminifera are in some cases partially replaced by authigenic minerals such as pyrite and glauconite. Taphonomic modification can also include dissolution and physical abrasion (especially in slowly accumulating sediments) and can alter the relative abundance of certain species (Stassen et al., 2015). In general, planktonic foraminifera and small, fragile benthics (e.g., hyaline biserial and triserial taxa and *Spiroloculina* sp.) are more prone to dissolution (Nguyen et al., 2009). The high percent planktonics in sequences E3–E7 suggests limited alteration by dissolution, although some dissolution may help account some of the unexplained percent planktonic variations. The transition to shallowest biofacies A across the E7-E8 sequence boundary which continues into sequence E10 is also associated with a dramatic drop in percent planktonics and ostracods; this could suggest some degree of post-depositional degradation due to physical reworking and breakage associated with shallower water depths. The increase in percent ostracod valves, which is a helpful taphonomic indicator of physical abrasion and amount of breakage (Cohen, 2003), suggests that Bass River sediments display a moderate degree of alteration, especially in shallower water depths.

Sequence Stratigraphy

We use benthic foraminiferal biofacies to reconstruct paleobathymetric changes, make inferences on systems tracts within these sequences (Fig. 3), and make comparisons to previously studied New Jersey coastal plain sites. Sequence boundaries identified in this paper have been defined previously, and unconformities are identified based on lithology and physical stratigraphy, including irregular contacts, reworking, gamma-ray peaks, bioturbation, and paraconformities inferred from biostratigraphic breaks (Miller et al., 1998b). In general, the Eocene section at Bass River is composed primarily of silty clays with variations arising mostly from changes to slightly sandy to very slightly sandy (slightly glauconitic or slightly quartzose). These minor sedimentological variations are interpreted as significant within a sequence stratigraphic context. Lithologic evidence presented here derives from the Bass River site report (Miller et al., 1998b), and we provide evidence to show similar relative depth trends between biofacies and lithofacies within each sequence.

Sequence E3

Greatest water depths are found in sequence E3 (corehole depth 337.9–299.1 m; 1108.5–981.3 ft; upper lower Eocene), which is dominated by biofacies D (125 ± 25 m water depth; Fig. 3). Sequence E3 deepens upsection (TST) to maximum water depths (~150 m) at the MFS, coinciding with the highest planktonic foraminiferal abundance (86%) and peak in *C. eocaenus* (one of the deepest-dwelling species in this section). Above the MFS, decreases in *C. eocaenus* and planktonic foraminiferal percentages indicate that sequence E3 shallows upsection, characteristic of HSTs. A contact at 299.1 m (981.3 ft) separates indurated clays below from characterized bioturbated silty clays above and is associated with a gamma-log peak, indicating the E3-E4 sequence boundary (Miller et al., 1998b). The average planktonic foraminiferal abundance for the eight samples analyzed in sequence E3 is high at 78%. The occurrence of biofacies D in sequence E3 at Bass River is further supported by the coeval occurrence of similar biofacies D and E of Browning et al. (1997a) at other New Jersey coastal plain sites (Island Beach and ACGS#4). Lowest percent coarse fraction (i.e., highest component of clay) and highest average number of whole ostracod carapaces (low percent single valves) further support deep water depths in sequence E3. In addition, the percent of single ostracod valves increases from ~70% at the base of E3 to ~90% at the top of E3, in agreement with our interpretation of shallowing upsection.

Sequence E4

Deep water depths continue in sequence E4 (corehole depth 299.1–292.56 m; 981.3–959.85 ft), which is characterized by biofacies D (125 ± 25 m water depth). The lithofacies in sequence E4 is dominated by marls with slight glauconite enrichment at the base (indicative of the TST; Miller et al., 1998b), and are consistent with the biofacies representing deposition in outer neritic (>100 m) paleodepths. Percent planktonic foraminifera decreases above the E3-E4 sequence boundary, and then increases upsection. The average planktonic foraminiferal abundance for the five samples analyzed from sequence E4 is 61%; changes in percent planktonics within this sequence may be due to preservation because the benthic biofacies indicates relatively uniform paleodepth (Fig. 3). *C. pseudoungerianus* decreases through sequence E4 with an increase in *C. micrus*, followed by a large decrease in *C. micrus* across the E4-E5 sequence boundary, indicating a change from deeper- to shallower-dwelling species across a sequence boundary. We also observe a coincident decrease in percent planktonics across the E4-E5 sequence boundary, from 74% to 34%.

Sequence E5

Sequence E5 (corehole depth 292.56–290.89 m; 959.85–954.35 ft) is very thin (1.68 m; 5.5 ft), is bracketed by hiatuses of ~0.5 and 2.0 m.y. (Fig. 2), is described as a glauconitic burrowed silty clay (Miller et al., 1998b), and is characterized by biofacies D (125 ± 25 m water depth). Although only two samples are examined within this thin sequence, we interpret a second peak in *C. eocaenus* to indicate a deepening upsection (TST) with maximum depths of 150 m. Average percent planktonics for sequence E5 is lower than in the previous two sequences, at 36%. While biofacies D is less important within sequence E5 than in the sequence below, and planktonics and ostracods are not particularly high, a significant peak in *C. eocaenus* (the deepest-dwelling species in our study) to ~20% is observed within E5. Sequence E5 at Island Beach and ACGS#4 is also characterized by coeval biofacies D of Browning et al. (1997a).

Sequence E6

Sequence E6 (corehole depth 290.89–284.07 m; 954.35–932 ft) is characterized primarily by biofacies B (75 ± 15 m water depth). A deepening-upward TST occurs at the base of E6, indicated by a peak in *C. pseudoungerianus* (an element of deeper biofacies D). Above this peak, shallower biofacies B and A dominate, indicating the shallowing-upward HST. Consistent with the biofacies, the lithofacies show basal slightly more glauconite-rich mud (deepening TST), which grades to medial silty clays (HST) to slightly glauconitic (possibly reworked) clays at the top of the sequence (Miller et al., 1998b). Sequence E6 is overall more carbonate rich than the underlying Manasquan sequences (E3–E4) with an upward trend of more carbonate in the sand fraction. The average planktonic foraminiferal abundance for the three samples analyzed in sequence E6 is 65%. Percent planktonics dramatically decreases from 77% to 37% across the E6-E7 sequence boundary, and although percent planktonics returns to 57% within sequence E7, this further supports a fall in sea level across the sequence boundary.

Sequence E7

Sequence E7 (corehole depth 284.07–269.99 m; 932–885.8 ft) is dominated by biofacies B (75 ± 15 m water depth). The abundance of deeper-dwelling *C. cocoaensis* delineates the basal MFS (100 m water depth). The basal TST and thick HST in the middle to upper part of the sequence are supported by lithology: a slight but notable increase in glauconite in the burrowed clays at the base of sequence E7 (TST) is overlain by decreasing glauconite as the section transitions upward from silty clays (lower HST) to slightly sandy clays (HST) with an increasing proportion of shell material (Miller et al., 1998b). Ten samples were analyzed from sequence E7, with an average planktonic foraminiferal abundance of 56%. Although little variation is observed within the middle section of E7, percent coarse fraction begins to increase in the upper section, indicative of shallowing upsection. We also note a significant decrease in percent planktonics across the E7-E8 sequence boundary from 45% to 16%. The average number of ostracods per sample decreases from 37 in sequences E3–E7 to 6 in sequences E8–E10.

Sequence E8

Minimum water depths of 60 m are interpreted in sequence E8 (corehole depth 269.99–263.23 m; 885.8–863.6 ft), based on the presence of biofacies A (60 ± 10 m water depth) with deeper biofacies C and B at the base (75 ± 25 m water depth). Here, the bioturbated silty clays of the lower Shark River Formation (sequences E5–E7) transition to the slightly glauconitic clays of the upper Shark River formation (sequences E8–E9) (Miller et al., 1998b). Sequence E8 has slightly glauconitic clays at the base (TST), medial clays (lower HST), and a slightly sandier upper section with quartz sand covarying with reworked glauconite (upper HST) and an upsection decrease in shells (Miller et al., 1998b). The increase in abundance of *Uvigerina* spp. (commonly found in TST) and peak in *S. claibornensis* (component of deeper biofacies C and D) indicate a deepening-upward basal TST to the MFS (75 m water depth at ~268 m corehole depth), although we do note that this is a very thin interval (<2 m). The basal TST and upper-section HST are also characterized by a switch from biofacies C (deeper) to biofacies A (shallower). A decrease in diversity indices and increase in the percent coarse fraction upsection further supports an overall shallowing-upward trend within sequence E8. In addition, higher benthics per gram at the base (deeper water depths) and decrease in number of benthics per gram in the upper half of the sequence supports shallowing upsection. Although we observe a peak in the number of benthics per gram within sequence E8, the general shallow-water depths for E8 are consistent with the low planktonic foraminiferal abundances (14%) and low ostracod abundances and diversity in this section. Similar water depths are found at the Atlantic City and Island Beach sites (75 ± 15 m), with biofacies comparable to biofacies A and B present within sequence E8 (Browning et al., 1997a).

Sequence E9

Similar to sequence E8, the base of upper Eocene sequence E9 (corehole depth 263.23–258.04 m; 863.6–846.6 ft) is characterized by a switch from biofacies C and B (75 ± 25 m water depth) to biofacies A (60 ± 10 m water depth), indicative of shallowing upsection. Glauconite and quartz sand are more abundant in sequence E9 than in any of the lower sequences. The deepest water depths in this sequence are indicated by the occurrence of glauconite, abundance increase in *Uvigerina* spp. and *S. claibornensis,* and peak in planktonic foraminiferal abundance, representing the deepening-upward basal TST. Above the MFS (75 m water depth at 262.5 m corehole depth), biofacies A dominates, indicating water depths of 60 m. Sequence E9 has a similar average planktonic foraminiferal abundance (15%) as in the previous sequence. We also observe a decrease in percent planktonics from 13% to 3% across the E9-E10 sequence boundary. In addition, the highest percent coarse fraction within this sequence further supports shallow water depths.

Sequence E10

Although only the lowermost section of upper Eocene sequence E10 (corehole depth 258.04–208.76 m; 846.6–684.9 ft) is shown in this study, E10 is characterized by biofacies A (60 ± 10 m water depth) and represents the shallowest sequence. In the basal 1.95 m (6.4 ft) of this sequence, two samples indicate a deepening-upward TST and abundance peak in the genus *Uvigerina*. The bottommost sample from sequence E10 shows the lowest percent planktonics (2.5%) found at Bass River, further supporting our conclusion that sequence E10 is the shallowest. In the base of sequence E10, two samples yield a very low average planktonic foraminiferal abundance of 6%. Low ostracod diversity and high (100%) percent valves from basal sequence E10 support our interpretation of the shallowest water depths found in this study.

Stable Isotopes

The $\delta^{18}O$ and $\delta^{13}C$ results from six species of benthic foraminifera (*A. wilcoxensis, A.* aff. *dissonata, C. cocoaensis, C. pippeni, C. eocaenus,* and *C. pseudoungerianus*) and two genera of planktonic foraminifera (*Acarinina* spp. and *Subbotina* spp.) are shown in Figure 12 to track sea level and paleoceanographic changes throughout our section. *Alabamina* and *Cibicidoides* are typically epifaunal genera (Thomas, 1990), although we find that our $\delta^{13}C$ values for the genus *Alabamina* are consistently lower by 0.63‰ than the *Cibicidoides* $\delta^{13}C$ values, suggesting that Alabamina was infaunal (at least shallow infaunal). The low $\delta^{13}C$ values in infaunal species result from higher organic carbon in the sediments arising from higher productivity in the surface waters and/or through an increase in preservation in sediments. Decay of buried organic matter (which is enriched in ^{12}C) depletes the porewaters of O_2 and releases the ^{12}C, which is then

incorporated into the tests of foraminifera. Therefore, we interpret early Eocene to early middle Eocene (corehole depth 282–312 m; 925–1025 ft) *Alabamina* as infaunal based on their lower $\delta^{13}C$ values compared to epifaunal *Cibicidoides*. Although there is a species offset, the $\delta^{13}C$ values of the different species track similar trends. Surface-dwelling *Acarinina* $\delta^{13}C$ values are consistently higher than the thermocline-dwelling *Subbotina* values (which are comparable to the *Cibicidoides* values), yet follow comparable trends.

Results from our $\delta^{13}C$ values from all species of benthic foraminifera show an overall decrease from the lower to the upper Eocene (Fig. 12). The $\delta^{13}C$ decreases occur in the upper sections of sequences E7, E8, and E9 (at corehole depths 270.36, 264.26, and 260.60 m, respectively; 887, 867, and 855 ft). The $\delta^{13}C$ decrease in the upper E7 sequence is also accompanied by an increase in abundance of *Spiroplectammina alabamensis*, an infaunal species (Fig. 5). We also show increases in $\delta^{13}C$ following the E7-E8, E8-E9 and E9-E10 sequence boundaries, which correspond with abundance increases in the genus *Uvigerina* (Figs. 3, 4).

The $\delta^{18}O$ values increase upsection at Bass River (Fig. 12). Increases in $\delta^{18}O$ occur across five out of the eight sequence boundaries (E2-E3, E4-E5, E5-E6, E7-E8, and E9-E10) we studied. The uncertainties in interpreting changes across these sequence boundaries associated with hiatuses are discussed below. A significant decrease in $\delta^{18}O$ (1.19‰) at corehole depth 274–270 m (900–885 ft) occurs leading into the E7-E8 boundary. Benthic foraminiferal $\delta^{18}O$ values are lowest in early Eocene sequence E2 (–3.25‰) and are consistently low throughout early Eocene sequences E3–E4, corresponding with the greatest water depths in our section (125 ± 25 m) and the EECO. *Acarinina* $\delta^{18}O$ values are lower than *Subbotina* and benthic (*Cibicidoides* and *Alabamina*) values, as expected for surface dwellers.

Mg/Ca Temperatures and $\delta^{18}O_{sw}$

Benthic and planktonic foraminiferal Mg/Ca samples are focused around select sequence boundaries (E2-E3, E4-E5, E5-E6, E6-E7) to evaluate if sea-level falls indicated by biofacies and lithofacies are associated with changes in $\delta^{18}O_{sw}$ associated with glaciation. Mg/Ca-derived temperature estimates from benthic foraminifera (bottom-water temperature, BWT; we use this term in the sense that benthic foraminifera record seafloor temperature) and planktonic foraminifera (sea-surface temperature, SST) are shown across these sequence boundaries in Figure 12. Planktonic foraminiferal SSTs are consistently warmer than benthic BWTs; both SST and BWT track similar trends. In addition, surface-dwelling *Acarinina* spp. SSTs are higher than thermocline-dwelling *Subbotina* spp. SSTs, as expected. We observe a 5.2 ± 1 °C decrease in SST from *Acarinina* and 3.8 ± 1 °C decrease from *Subbotina* across the E4-E5 sequence boundary. *Cibicidoides pseudoungerianus* BWT remains constant across the E2-E3 sequence boundary but decreases 2.3 ± 1 °C immediately above the sequence boundary. BWT decreases 3.8 ± 1 °C across the E4-E5 sequence boundary (approximately the lower Eocene–middle Eocene boundary), followed by an increase and then decrease of 3 ± 1 °C within sequence E5. Little temperature change is associated with sequence boundaries E5-E6 and E6-E7 from either the benthic or planktonic foraminifera. Overall, warmer temperatures are recorded in the Manasquan Formation (lower Eocene) compared to the lower Shark River Formation (middle Eocene). $\delta^{18}O_{sw}$ values increase across the E2-E3 and E5-E6 sequence boundaries (Fig. 12), but are equivocal across the E4-E5 and E6-E7 sequence boundaries (see Discussion).

DISCUSSION

Stable Isotopes

Benthic and planktonic foraminiferal stable isotopes provide the means to reconstruct paleoceanographic changes during the early Eocene to early late Eocene at Bass River (Fig. 12). $\delta^{13}C$ decreases occur in the upper portions of sequences E7, E8, and E9 (Fig. 12). The decreases in $\delta^{13}C$ at Bass River correspond to global decreases in $\delta^{13}C$ in the upper sections of sequences E7 and E8, though the $\delta^{13}C$ decrease in sequence E9 is much larger than in deep-sea benthic foraminiferal records (Fig. S2 [footnote 1]). The decrease in $\delta^{13}C$ values in the upper E7 sequence is accompanied by an increase in *S. alabamensis* abundance (Fig. 5). *Spiroplectammina* is an infaunal genus (Peryt et al., 1997) and we interpret it as indicating an increase in productivity. During periods of high (seasonal) productivity, an influx of organic matter is delivered to the ocean sediments, which when oxidized releases ^{12}C that drives down pore-water $\delta^{13}C$. This $\delta^{13}C$ decrease also corresponds with a $\delta^{18}O$ decrease. We speculate that this $\delta^{18}O$ decrease can be attributed to riverine input, which supplies nutrients and stimulates productivity and/or an increase in temperature. This significant absolute decrease in $\delta^{13}C$ (1.4‰) and $\delta^{18}O$ (1.2‰) across corehole depths 274.3 m (900 ft) to 270.4 m (887.3 ft) matches the global signal, yet the magnitude is higher at Bass River (Fig. 13; Fig. S2 [footnote 1]), further supporting some regional component, such as a change in productivity. The increases in the $\delta^{13}C$ values following the E7-E8, E8-E9 and E9-E10 sequence boundaries correspond with abundance increases in the genus *Uvigerina* (Fig. 4). An increase in *Uvigerina* spp. typically corresponds with deepening-upward TSTs (e.g., Loutit et al., 1988), which we find at the base of sequences E8, E9, and E10 (Fig. 3). The corresponding abundance increase in the genus *Uvigerina* and $\delta^{13}C$ values is puzzling, as *Uvigerina* is an infaunal species and commonly indicates an increase in productivity.

Superimposed on the overall $\delta^{18}O$ increase and cooling trend following the EECO, a transient $\delta^{18}O$ minimum is observed globally at ca. 41 Ma (Fig. 13), called the MECO warming event (Bohaty and Zachos, 2003). Based on our age model at Bass River, the MECO event likely is not recorded due to the unconformity at the E8-E9 sequence boundary. In order to confirm the absence or presence of the MECO event, higher-resolution sampling across this interval is needed.

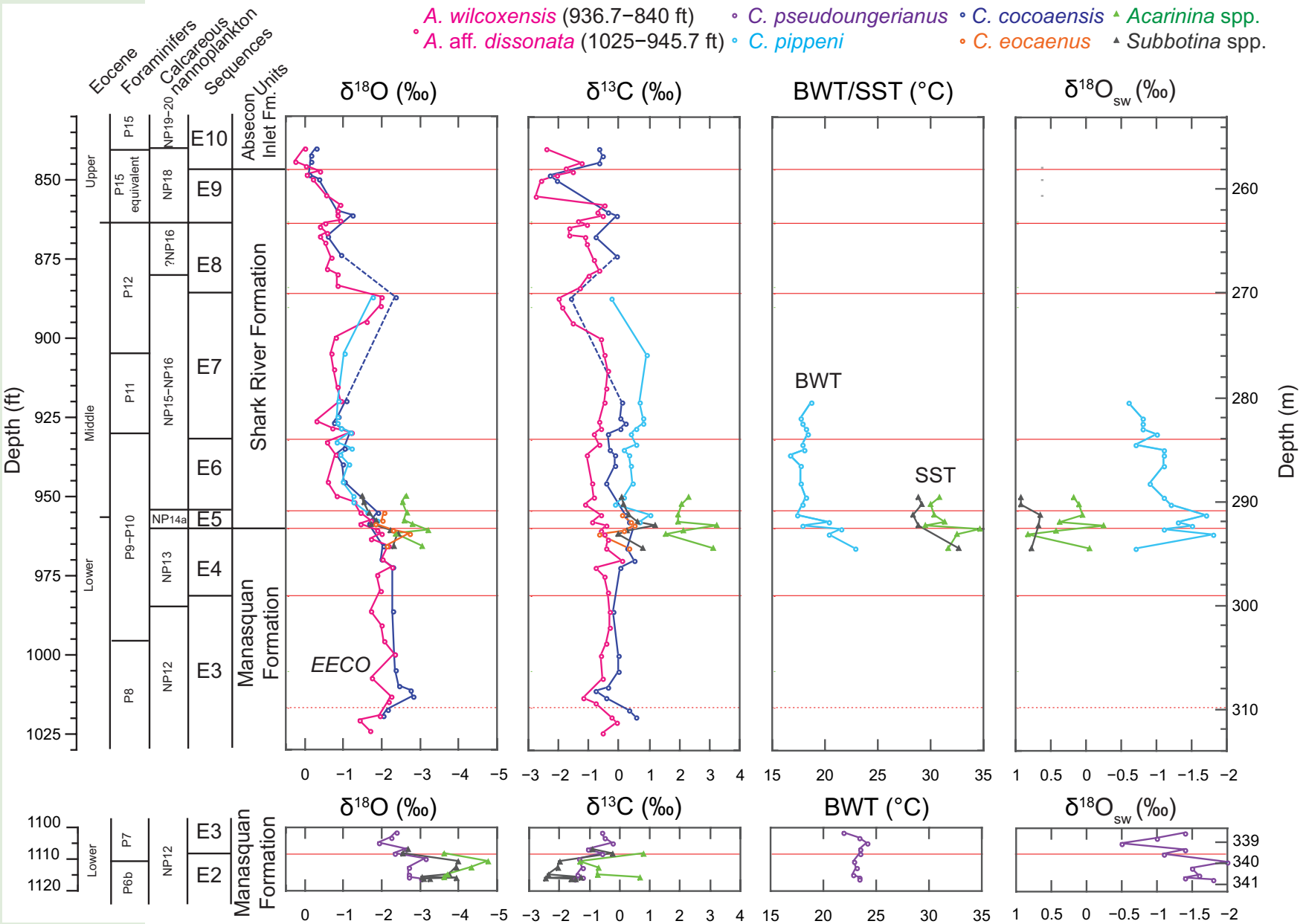

Figure 12. Stable isotopes ($\delta^{18}O$ and $\delta^{13}C$), Mg/Ca temperature reconstructions (BWT—bottom-water temperature; SST—sea-surface temperature), and $\delta^{18}O_{sw}$ (seawater) estimates from benthic and planktonic foraminifera from sequences E2–E10 at Bass River, New Jersey coastal plain (USA). Genera abbreviations: A.—Alabamina; C.—Cibicidoides. The Early Eocene Climatic Optimum (EECO; ca. 52–50 Ma) event is labeled.

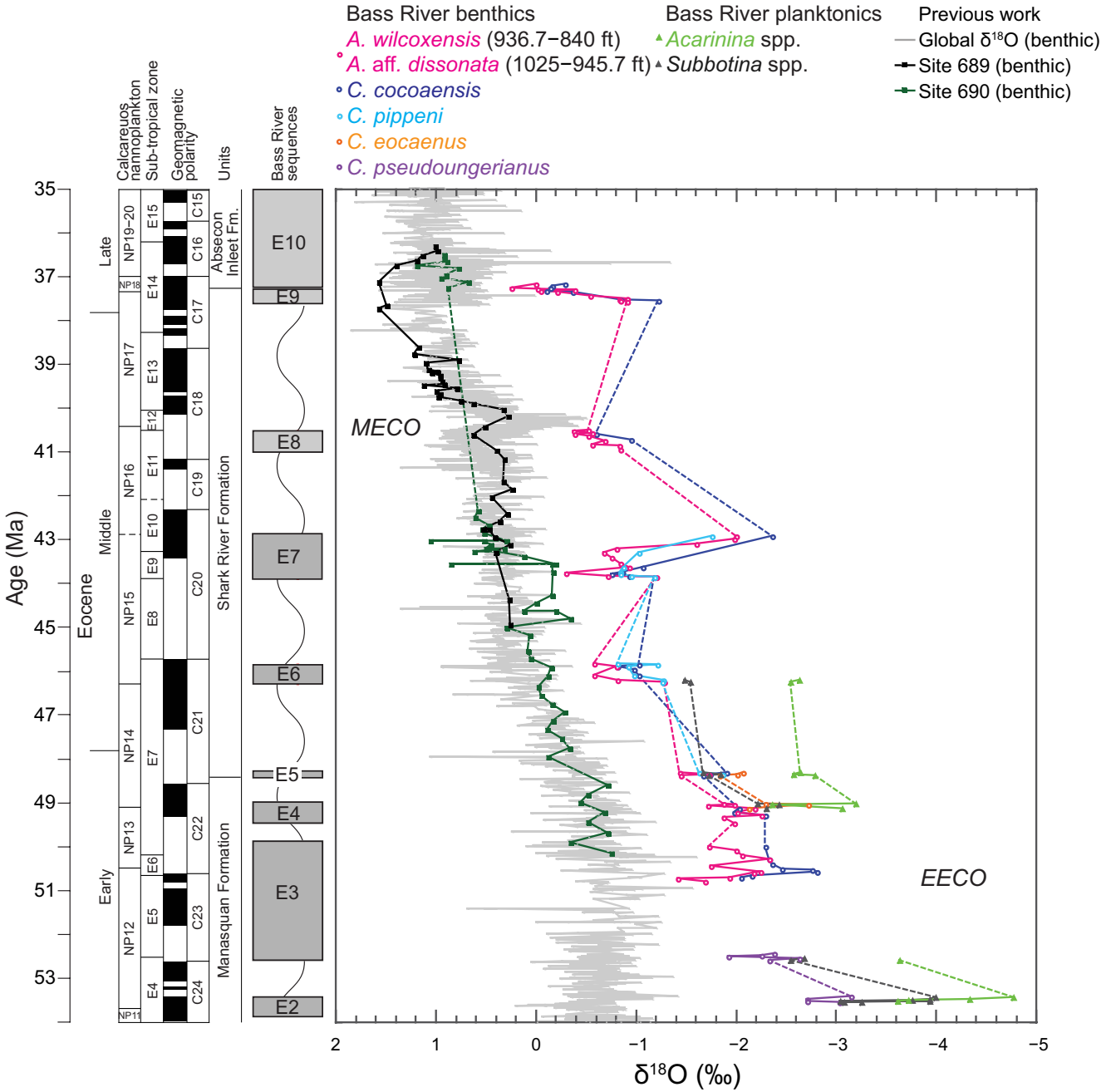

Figure 13. Comparison of benthic and planktonic foraminiferal $\delta^{18}O$ (this study, New Jersey coastal plain, USA) with the benthic global $\delta^{18}O$ (gray line; Cramer et al., 2009) and benthic $\delta^{18}O$ records from the Southern Ocean (Ocean Drilling Program Sites 689 [black line] and 690 [green line]; Kennett and Stott, 1990). Genera abbreviations: A.—Alabamina; C.—Cibicidoides. Wavy lines indicate hiatuses in Bass River sequences. The Middle Eocene Climatic Optimum (MECO; ca. 41 Ma) and the Early Eocene Climatic Optimum (EECO; 52–50 Ma) are labeled based on the global records. The time scale of Gradstein et al. (2012) is used throughout.

Evidence for Glacioeustasy

Based on our integrated analysis of physical stratigraphy, microfossils, and geochemistry, we interpret the Eocene Bass River section to reflect GMSL changes that are driven by ice-volume variations. We compare our benthic and planktonic foraminiferal $\delta^{18}O$ data with global benthic foraminiferal $\delta^{18}O$ trends (Cramer et al., 2009) and benthic foraminiferal $\delta^{18}O$ records from the Southern Ocean (ODP Sites 689 and 690; Kennett and Stott, 1990) (Fig. 13). Although our isotope trend provides snapshots of ocean history during periods of high sea level recorded in the sedimentary record, overall $\delta^{18}O$ values increase upsection at Bass River (Figs. 12 and 13), consistent with global cooling (Cramer et al., 2009). As expected, our shallow-water benthic and planktonic $\delta^{18}O$ values are consistently lower by 0.5‰–1.5‰ than the deep-sea benthic foraminifera from Antarctic ODP Sites 689 and 690, reflecting 2–6 °C cooler temperatures in the bathyal zone at those sites (Eocene water depths of ~1400 m and ~2250 m, respectively; Kennett and Stott, 1990), yet they track similar patterns throughout our section, indicating that Bass River isotopes record a global signal.

The greenhouse conditions of the Eocene are presumed to have been largely ice free with modern-sized Antarctic glaciation occurring at 33.8 Ma (e.g., Miller et al., 1991; Zachos et al., 1996). Miller et al. (1998a) showed that all but two latest Eocene–middle Miocene onshore New Jersey sequence boundaries are associated with increases in $\delta^{18}O$, suggesting a link between sequence boundaries and a drop in sea level caused by glacioeustasy. Furthermore, Miller et al. (1998a) proposed that small-amplitude sea-level changes (<20 m) associated with the growth and decay of small ice sheets ($8–12 \times 10^6$ km^3 [20–30 m glacioeustatic equivalent]; DeConto and Pollard, 2003b) appear to correlate with $\delta^{18}O$ increases in the early to middle Eocene, a time interval previously thought to have been ice free. In order to reconcile warm high-latitude climates coinciding with deep-sea $\delta^{18}O$ increases and eustatic falls, Miller et al. (2005b) proposed that Late Cretaceous to Eocene ice sheets (which only existed during Milankovitch insolation minima, lasting ~100–200 k.y.) did not reach the Antarctic coast. These small ice caps in the interior of Antarctica allowed coastal Antarctica to remain warm, yet still allowed for changes in sea level due to glaciation (Miller et al., 2005b).

Here, we use $\delta^{18}O$ and Mg/Ca to reconstruct temperature and $\delta^{18}O_{sw}$ across multiple Bass River sequence boundaries in the early to middle Eocene to resolve whether relative sea-level falls (observed as water-depth changes) are associated with glaciation. Benthic foraminiferal $\delta^{18}O$ values increase across five out of the eight Eocene sequence boundaries studied (E2-E3, E4-E5, E5-E6, E7-E8, and E9-E10; Fig. 12; Table 1). Values decrease across sequence boundaries E6-E7 and E8-E9, but increase immediately above (Fig. 12; Table 1). Where planktonic $\delta^{18}O$ data are available, they show similar increases at sequence boundaries (E4-E5 and E5-E6; Fig. 12; Table 1). Although the record at Bass River is less continuous and punctuated by hiatuses, these $\delta^{18}O$ increases are also observed in deep-sea benthic foraminiferal records (Fig. 13; Cramer et al., 2011), supporting that the global signals are recorded at Bass River. Although the Bass River data are generally sparse and hiatuses associated with them are long in certain cases, they do show 0.3‰–1.2‰ increases across sequence boundaries, which we associate with glacial lowerings of sea level. The $\delta^{18}O$ changes are similar to those reported by Browning et al. (1996) from previous deep-sea studies (Table 1).

Middle Eocene and younger sea-level changes respond on Milankovitch scales, paced primarily by the 1.2 m.y. tilt cycle, though the forcing on early Eocene changes is not certain (Boulila et al., 2011). Higher-order cycles (400, quasi-100, 41, 23, and 19 k.y.) are difficult to resolve in the New Jersey coastal plain due to moderate sedimentation rates (40 m/m.y.) and long hiatuses. Though hiatuses across middle Eocene sequences are long, our data show that they are associated with million-year-scale ice-volume increases, presumably on the 1.2 m.y. scale. We suggest that the shorter hiatuses in the early Eocene are the result of lower-amplitude sea-level variations as implied by our data. The cause of these early Eocene greenhouse sea-level variations has been debatable, though our data suggest that they were glacioeustatically forced, again presumably on the 1.2 m.y. scale.

Difficulties in using the stratigraphic record at Bass River to study changes in sea level arise from the lack of sediment preserved during long hiatuses. Of the five sequence boundaries that show an increase in $\delta^{18}O$ values, three occur across short hiatuses (E2-E3, E4-E5, and E9-E10) and two over long hiatuses (E5-E6 and E7-E8). Two of the sequence boundaries that show a decrease in $\delta^{18}O$ (E6-E7 and E8-E9) occur across the longest hiatuses observed in our studied interval. Changes observed across shorter-duration hiatuses (E2-E3, E3-E4, E4-E5, and E9-E10 sequence boundaries) provide firm evidence for a link of sequence boundaries and ice volume, even in the early Eocene greenhouse-doubthouse world. Sequence boundaries associated with longer hiatuses, such as the $\delta^{18}O$ decrease at the E8-E9 sequence boundary, potentially reflect snapshots in each of these short sequences of the overall global $\delta^{18}O$ trend and may represent more than one sea-level event. The incompleteness of parts of the Bass River record makes it hard to say for certain that all stratigraphic changes can be explained by glacioeustasy. We can be more confident in our interpretation of a glacioeustatic link where we observe increases in $\delta^{18}O$ across short hiatuses. Although not inconsistent, increases in $\delta^{18}O$ across sequence boundaries represented by longer hiatuses may be more difficult to tie reasonably to a specific glacioeustatic event.

Sea-level calibrations using $\delta^{18}O$ variations at Bass River are not straightforward due to three effects: (1) changes in water depth; (2) freshwater input; and (3) uncertainties in $\delta^{18}O_{sw}$-sea level calibration. The amplitudes of $\delta^{18}O$ increases at Bass River are similar to changes noted in deep-sea $\delta^{18}O$ records at ca. 49 Ma (E4-E5 sequence boundary), 46–47 Ma (E5-E6), and 42 Ma (E7-E8; Fig. 13; Table 1). Though $\delta^{18}O$ values decrease across the E6-E7 sequence boundary, the increase captured at the base of E7 correlates with a ca. 44 Ma global $\delta^{18}O$ increase. The $\delta^{18}O$ decrease in sequence E7 and the increase across the E9-E10 sequence boundary appear amplified relative to deep-sea records and may reflect effects of water depth or freshwater input, supported by foraminiferal and sedimentological evidence (discussed below). Therefore, $\delta^{18}O$ variations observed at Bass River generally mimic global records; coupled with Mg/Ca, they provide a first-order correlation of sequence boundaries and $\delta^{18}O_{sw}$ (we discuss complications due to water depth and freshwater input below).

TABLE 1. FLUCTUATIONS IN $\delta^{18}O$ and $\delta^{18}O_{sw}$ (SEAWATER), CORRESPONDING CHANGES IN SEA LEVEL (SL), AND Mg/Ca-DERIVED TEMPERATURE RECONSTRUCTIONS ARE SHOWN ACROSS SEQUENCE BOUNDARIES AT BASS RIVER (NEW JERSEY COASTAL PLAIN, USA) AND ARE COMPARED TO THE WORK OF BROWNING ET AL. (1996)

Sequence boundary	Hiatus age (Ma)	$\Delta\delta^{18}O_{bf}$ (‰) Browning et al. (1996)	ΔSL (m) Browning et al. (1996)	$\Delta\delta^{18}O_{bf}$ (‰) this study	Comment	ΔSL (m) 0.11‰/10 m 66% ice	ΔSL (m) 0.10‰/10 m 33% ice	ΔMg/Ca temperature (°C)	$\Delta\delta^{18}O_{sw}$ (‰) this study	ΔSL (m) 0.10‰/10 m	ΔSL (m) 0.13‰/10 m
E9-E10	37.3	–	–	0.5	Bf increase across SB 0.4‰–0.6‰	30	17	–	–	–	–
E8-E9	40.5–37.6	0.3	27	–0.4	Bf decrease across SB, increase above and below	–24	–13	–	–	–	–
E7-E8	42.9–41.0	0.25	23	1.2	Increase across SB; accentuated by local effects	72	40	–	–	–	–
E7 base	ca. 41	–	–	0.6	Bf and pf increase immediately above SB	36	20	+0.5	0.7	73	56
E6-E7	45.8–43.9	0.3	27	–0.3	Bf and pf decrease across SB; 0.4‰–0.9‰ increase immediately above	–18	–10	+0.6	–0.2	–15	–12
E5-E6	48.3–46.3	0.2	18	0.3	2 m.y. hiatus; bf and pf 0.2‰ increase at SB; bf and pf ~0.4%‰ increase immediately above	18	10	+0.3 to +0.8	0.4	44	34
E4-E5	49.0–48.4	–	–	0.5	Bf and pf increase across SB 0.4‰–0.6‰	30	17	–2.5 to –5.2	–0.1	0	0
E3-E4	49.9–49.5	–	–	–	Insufficient data	–	–	–	–	–	–
E2-E3	53.4–52.6	–	–	0.7	Bf average increase across SB	42	23	+0.6	0.9	85	65

Notes: We calculate changes in sea level from $\delta^{18}O$ using: (1) the late Pleistocene calibration of 0.11‰/10 m with 67% due to ice and 33% due to temperature (Fairbanks, 1989); and (2) the Late Cretaceous and Campanian–Maastrichtian calibration of 0.10‰/10 m using 25%–33% ice volume and 66%–75% temperature (Miller et al., 2005a). $\delta^{18}O_{sw}$ sea level and Mg/Ca-derived temperature reconstructions are shown across specific sequence boundaries and the corresponding ΔSL. The low-end-member estimates from Winnick and Caves (2015) using 0.13‰/10 m are also shown. Dashes indicate where no increase or decrease in $\delta^{18}O$ is observed. The time scale of Gradstein et al. (2012) is used throughout. SB—sequence boundary; bf—benthic foraminiferal; pf—planktonic foraminiferal.

Though we provide estimates of changes in $\delta^{18}O_{sw}$ (Fig. 12), the $\delta^{18}O_{sw}$–sea level calibration is uncertain. The Pleistocene $\delta^{18}O$–sea level calibration (0.11‰/10 m, with 67% due to ice and 33% due to temperature; Fairbanks and Mathews, 1978; Fairbanks, 1989) is most likely not applicable for the warmer temperatures of the Eocene (Miller et al., 2005b). Therefore, we compare sea-level changes using the Pleistocene calibration and the Oligocene calibration of 0.10‰/10 m (Pekar et al., 2002). We also include sea-level approximations using Late Cretaceous and Campanian–Maastrichtian estimates of 25%–33% ice volume and 66%–75% temperature (Miller et al., 2005a). The low-end-member estimates from Winnick and Caves (2015) using 0.13‰/10 m are also shown in Table 1. These changes in sea level due to ice-volume variations are not true eustatic estimates though, because we did not take into account the processes that change ocean-basin volume, such as tectonoeustasy and crustal shortening (Miller et al., 2005a). Our estimates of sea-level lowerings are minima due to hiatuses and the absence of lowstand deposits in our section of Bass River, where the amount of lowering is unconstrained, possibly as the result of exposure and/or downward slope transport.

Our $\delta^{18}O$-based estimates for sea-level fall due to changes in ice volume show a wide range (Table 1), though our best estimate is ~20–25 m with a likely upper limit of 40 m (Table 1). In general, our sea-level changes are in agreement with Browning et al. (1996) when using the Oligocene calibration of 0.10‰/10 m, although we observe $\delta^{18}O$ increases across sequence boundaries E2-E3, E4-E5, and E9-10, and Browning et al. (1996) did not. Although the E7-E8 hiatus is ~2 m.y., representing a considerable gap in time in preserved section, we do observe a significant shift from biofacies B to shallower biofacies A and a major drop in percent planktonics and preserved ostracods. This significant environmental change that impacted both the surface and bottom waters at ca. 41 Ma may be the localized effects of the MECO event. In addition, much of the large $\delta^{18}O$ increase across the E7-E8 boundary (1.2‰) is likely attributable to regional cooling. The $\delta^{18}O$ increase across the E2-E3 sequence boundary is large (0.7‰), with ~40 and 20 m sea-level falls estimated using the Pleistocene and Cretaceous calibrations, respectively (Table 1), though we favor the lower estimate using a larger temperature component than in the Pleistocene.

We also present Mg/Ca-derived temperature and $\delta^{18}O_{sw}$ reconstructions across three sequence boundaries (Table 1). This approach yields very high ice-volume growth (sea-level falls as large as 85 m; Table 1). However, $\delta^{18}O$-Mg/Ca–based eustatic estimates have large uncertainties on individual peaks (±15–25 m; Miller et al., 2012), which may explain these high amplitudes. We conclude that the amplitudes of sea-level falls in the Eocene are still poorly known, but are likely on the order of 20–25 m, and are lower than icehouse falls of the Oligocene and younger (~50–60 m; Miller et al., 2005a, 2005b).

Bass River sequences are compared to previously studied New Jersey onshore boreholes of Browning et al. (1996) and to the sea-level curves of Haq et al. (1987), Miller et al. (2005a), and Kominz et al. (2008) (Fig. 14). Sites ACGS#4, Island Beach, and Atlantic City are recalibrated to the time scale of Gradstein et al. (2012) using updated age-depth plots for each site (Figs. S3–S5 [footnote 1]). Paleodepth estimates from our study are compared to those of these previously studied New Jersey sites and arranged along a depth gradient. The eustatic record of Haq et al. (1987) digitized and reproduced by Miller et al. (2005a), and backstripped sea level records of Miller et al. (2005a) and Kominz et al. (2008), are also shown, updated to the Gradstein et al. (2012) time scale.

With the possible exception of sequence E9, which is poorly dated at Bass River, the sites show coeval hiatuses, indicating that the attendant unconformities were associated with regional base-level lowerings. Based on foraminiferal

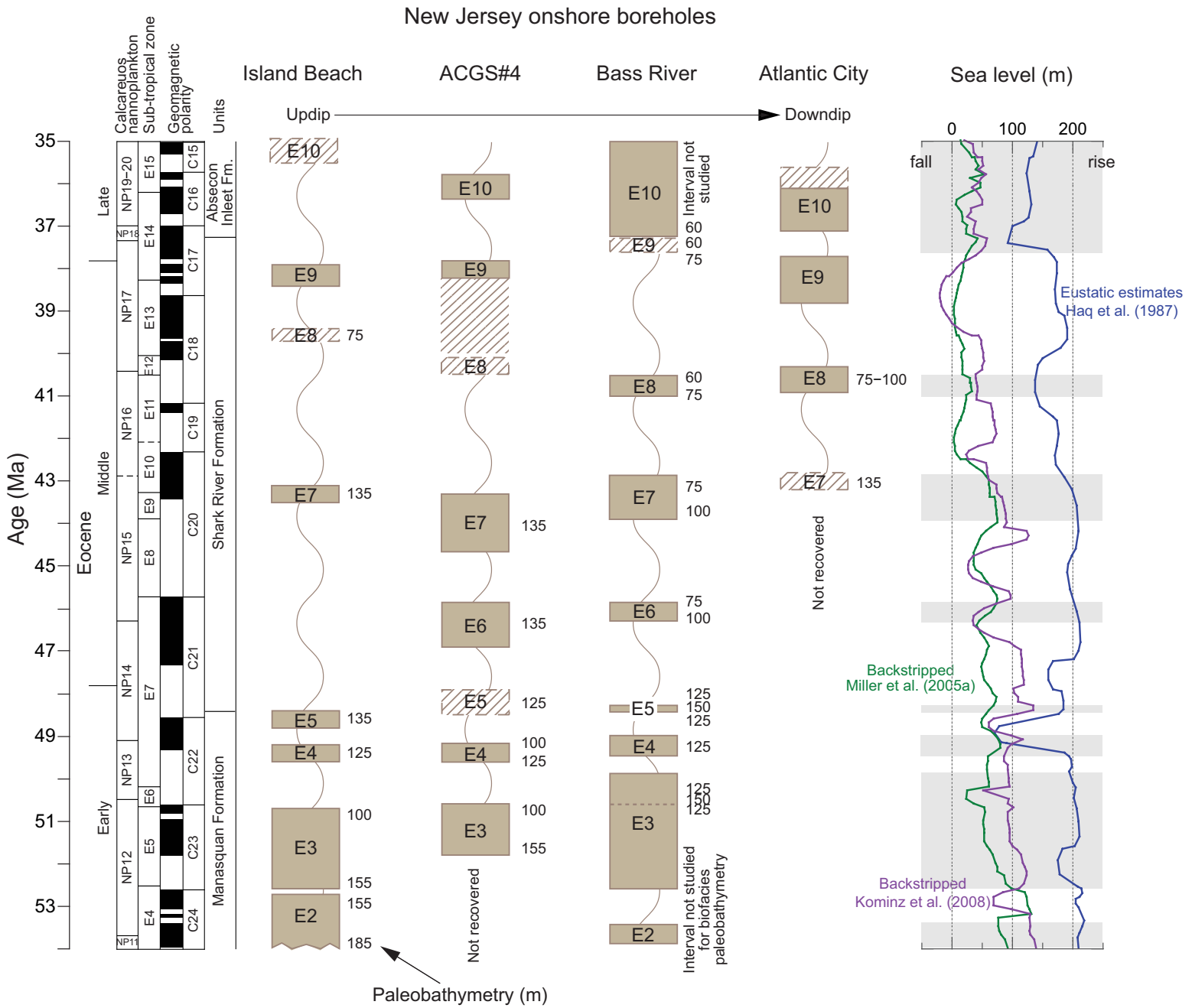

Figure 14. Bass River units (this study) compared to previously studied New Jersey coastal plain boreholes (Browning et al., 1996) and the sea-level curves of Haq et al. (1987), Miller et al. (2005a), and Kominz et al. (2008). The sea-level records of Miller et al. (2005a) and Kominz et al. (2008) include estimated lowstands. Paleodepths are inferred using benthic foraminiferal biofacies, where documented. Wavy lines indicate unconformities. Diagonal lines in sequences represent uncertainties in age. Gray shaded bars on the sea-level curve represent the studied interval at Bass River. Dashed line within sequence E3 indicates an unresolvable contact and may represent a sequence boundary (Miller et al., 1998b). The time scale of Gradstein et al. (2012) is used throughout.

biofacies, Bass River paleodepths are comparable to those of previously studied New Jersey boreholes, with paleodepths being the greatest in the lower Eocene and decreasing upsection. Although the Bass River, ACGS#4, and Island Beach sites essentially are located along a similar basin gradient (Fig. 1), deviations in paleobathymetry recorded among these sites within certain sequences can be attributed to differences in sediment supply along a strike line during these time periods. For example, we suggest that paleodepths in sequences E6–E7 were 35–60 m shallower than in the older study of Browning et al. (1996). Furthermore, no one site preserves the entire Eocene record, with hiatus durations varying among sites. Therefore, the discrepancies in paleobathymetry (specifically at sequences E6 and E7) may also result at least in part from the varying sequence duration recorded at each site (i.e., sequences do not necessarily perfectly overlap), and not all sequences record a basal TST or MFS. An unresolvable contact that may represent a sequence boundary at ca. 51 Ma (Miller et al., 1998b) could explain the location of the MFS at Bass River (as indicated by a peak in *C. eocaenus*) and differences in paleobathymetry between Bass River and sites from previous studies within sequence E3.

Compared to these previously analyzed boreholes, our study more closely reflects the backstripped sea-level curves, confirming the accuracy of our record. Bass River paleobathymetry estimates are in line with the backstripped sea-level curves (especially Kominz et al., 2008) at sequences E4, E5, and E7–E10. Slight disagreements occur within sequences E3 and E6. This may be attributed to the inclusion of estimated lowstands in the sea-level records of Miller et al. (2005a) and Kominz et al. (2008). Similarities between the New Jersey records (boreholes and backstripped sea-level curves) and the Haq et al. (1987) eustatic record suggest that early Eocene sequence boundaries are global (i.e., unconformities correspond with eustatic sea-level falls), although the amplitudes of the Haq et al. (1987) global sea-level events are too high by a factor of ~2–2.5 (Pekar et al., 2002; Miller et al., 2005a, 2011; John et al., 2011). These New Jersey sequences are marked with unconformities, with no one site providing a complete picture of sea-level history. Although significant gaps due to long middle Eocene hiatuses still exist, integrating Bass River with previously studied boreholes and eustatic estimates shows that million-year-scale sea-level falls likely caused widespread erosion across the paleoshelf (Fig. 14).

A 25–40 m sea-level fall would have only partially exposed the paleoshelf to subaerial erosion. Assuming gradients of 1:500–1:1000 observed in two-dimensional backstripping (Steckler et al., 1999) and the modern shelf would predict only exposure of 25–80 km of this wide (>>100 km) paleoshelf. There is little evidence for subaerial exposure at Bass River. However, a rapid (>>25 m/m.y.) glacioeustatic fall would have caused hiatuses across the paleoshelf due to submarine erosion and bypass. The extent of erosion and bypass would likely be related in part to the amplitude and rate of sea-level falls, with the longer middle Eocene hiatuses reflecting more severe sea-level falls.

The decrease in $\delta^{18}O$ from corehole depth 274–270 m (900–885 ft) in the upper part of sequence E7 is antithetical to other global records (Fig. 13) and highlights uncertainties in stable isotopic studies on shelf sections due to two effects, increases in river input and changes in water depth. The decrease in $\delta^{18}O$ could also have been due to influence of riverine waters, which have a lower $\delta^{18}O$ signature because of Raleigh fractionation associated with evaporation and/or precipitation. An increase in freshwater input via rivers during sea-level falls can decrease the local $\delta^{18}O$ values of the ocean water, though this effect is generally restricted to the inner shelf (<30 m) even in high-input environments such as the modern Amazon (Geyer et al., 1996), and the presence of abundant planktonic foraminifera argue against a low-salinity (i.e., lower than mean ocean by 1‰–2‰) surface water plume. Nevertheless, the input of isotopically light waters into the surface waters and bottom through sediment-laden freshwater can result in a low-salinity bottom layer that potentially explains the ~1‰ local $\delta^{18}O$ changes from sequence E7 to sequence E8 (Fig. 12), analogous to influences of meltwater in the Pleistocene Gulf of Mexico (e.g., Levanter et al., 1982). Freshwater input would have resulted in stratification associated with low $\delta^{13}C$ values, abundant infaunal *S. alabamensis*, and bioturbated clays observed in the upper section of sequence E7. We note that this anomaly appears to be the only major change potentially attributable to riverine change, because other $\delta^{18}O$ variations faithfully mimic global $\delta^{18}O$ changes (Fig. 13).

Benthic and planktonic foraminifera record a substantial increase in $\delta^{18}O$ (0.81‰–1.4‰) across the E2-E3 sequence boundary at ca. 52 Ma (Figs. 12, 13). No change in BWT is observed, providing evidence of glacioeustasy in the early Eocene. This increase in $\delta^{18}O$ at Bass River corresponds with a ~65 m fall in sea level documented in the backstripped sea-level curves of Kominz et al. (2008). Importantly, all of the change in sea level occurs during the E2-E3 hiatus at Bass River. Although detailed micropaleontological studies were not analyzed for this section, quantitative foraminiferal abundances on the samples bracketing the E2-E3 boundary at Bass River show a similar shallowing (see Table S1 [footnote 1]). Specifically, the abundance of *Trifarina wilcoxensis* (a component of biofacies H of Browning et al. [1997a] and indication of paleodepths of 185 ± 25 m) decreases from 79% to 3% across the E2-E3 boundary. *Cibicidoides micrus*, *C. pseudoungerianus*, and *C. eocaenus* (components of our biofacies D and indication of paleodepths of 125 ± 25 m) begin to dominate in the base of sequence E3. Therefore, we show a major (60 ± 25 m) decrease in water depth coupled with an increase in $\delta^{18}O$ across the E2-E3 sequence boundary during the early Eocene. This startling conclusion is derived from and supported by both regional water-depth studies and geochemical proxies, and indicates significant ice growth even in the "greenhouse" early Eocene.

Temperature reconstructions from both planktonic and benthic foraminifera show cooling across the E4-E5 sequence boundary (Fig. 12). Although there is a species offset between the benthic and planktonic foraminifera, the magnitude of cooling is similar. The slightly greater cooling illustrated by planktonic species indicates greater temperature changes in surface waters than at the seafloor.

Our BWT and SST reconstructions are comparable to a TEX_{86}^{H} temperature record from low-latitude Atlantic sites in the Eocene by Inglis et al. (2015) (Fig. S6 [footnote 1]). We demonstrate that our SST record at Bass River is similar to absolute temperatures measured by TEX_{86}^{H}, most importantly at South Dover Bridge, an Atlantic Coastal Plain site similar to Bass River. This

further validates our Mg/Ca BWT-SST reconstructions and interpretation for a decrease in temperature associated with a sequence boundary ca. 49 Ma.

Cooling continues into the upper E4 sequence, paired with an increase in $\delta^{18}O_{sw}$ and a decrease in water depth across the E5-E6 sequence boundary. An increase in $\delta^{18}O_{sw}$ and decrease in water depth continues within sequence E6, although we do not observe a change in temperature. This decoupling of temperature and $\delta^{18}O_{sw}$ could be the result of mid-latitude temperatures remaining constant as ice volume increased or the input of freshwater via rivers increased. A thin sequence E5, with absence of lowstand deposits, causes some ambiguity in the data presented (decreases in temperature across the E4-E5 sequence boundary [approximately the early Eocene–middle Eocene boundary] coupled with decreases in $\delta^{18}O_{sw}$). Although sequence E5 records only a brief interval of deposition and the E5-E6 hiatus is relatively long, the overall change in temperature and water depth from the top of sequence E4 to the base of E6 shows a 3.5–4.7 °C cooling and a fall in sea level of 25–50 m starting at 49 Ma. Further sampling may resolve some of the variability, although even the largest of samples did not contain sufficient specimens for single-species analysis and/or additional geochemical analyses. The report of IRD near Antarctica at ca. 49 Ma (Birkenmajer, 1988) further supports our interpretation of glacial growth and decay across the early Eocene–middle Eocene boundary.

The fall in sea level across the E2-E3 sequence boundary at ca. 52 Ma and cooling recorded across the E4-E5 sequence boundary at ca. 49 Ma occur during some of the shortest hiatuses in our studied interval, providing a firm link of sequence boundaries and $\delta^{18}O$ changes. In this paper, we propose that glacioeustatic changes occurred in the early Eocene, a time period previously believed to have been largely ice free. These interpretations are supported by micropaleontological paleobathymetry, stable-isotope analyses, and Mg/Ca temperature reconstructions. We show that even in these relatively warm climates, changes in sea level due to glacioeustasy likely existed. Limitations to our study arise from: (1) the shallow location of the onshore sequences on the continental shelf, restricting sediment preservation to times of higher sea level; and (2) the low resolution around sequence boundaries and relatively long hiatuses recorded in these New Jersey boreholes. To address these limitations, we present supporting geochemical evidence that indicates the growth and decay of small ice sheets during a cooling trend beginning in the early Eocene (at ca. 52 Ma). This cooling trend continued into the late Eocene, leading into the EOT and initiation of continental-sized Antarctic ice sheets.

CONCLUSIONS

Eight previously defined lower Eocene to lower upper Eocene sequences are resolved at Bass River using benthic foraminiferal assemblages, planktonic foraminiferal abundances, ostracod generic diversity, and lithologic changes. Four discrete benthic foraminiferal biofacies, delineated by factor analysis, represent paleo–water depths that allow for the interpretation of systems tracts within many of the sequences. Sequences at Bass River are dominated by thin basal deepening-upward TSTs overlain by shallowing-upward HSTs; LSTs have not been detected. The greatest water depths are found in lower Eocene sequence E3 (Manasquan Formation), which also correspond with the greatest planktonic foraminiferal abundance in the section. Shallowest water depths are obtained in late middle Eocene to late Eocene sequences E8–E10 (upper Shark River Formation) and are reflected in a significant biofacies shift, decrease in planktonic foraminiferal abundance, decrease in number of ostracods, and decrease in ostracod diversity.

The $\delta^{18}O$ and $\delta^{13}C$ are analyzed from six benthic foraminifera species (of the genera *Cibicidoides* and *Alabamina*) and two planktonic genera (*Acarinina* and *Subbotina*) to gain information on paleoceanographic change during this time period and provide a stable-isotope record from a benthic foraminiferal genus that has not been previously used. The overall decrease in $\delta^{13}C$ includes intervals of negative isotope excursions, which could be the result of global productivity increases. Species offsets due to microhabitat preferences could indicate an infaunal preference for the genus *Alabamina* during the Eocene. An overall increase in $\delta^{18}O$ following the EECO agrees with the global signal and the associated cooling trend.

A low-resolution study of temperature and $\delta^{18}O_{sw}$ reconstructions from benthic and planktonic foraminiferal Mg/Ca and $\delta^{18}O$ studies show a fall in sea level in the early Eocene at ca. 52 Ma and a ~4 °C cooling in the late early Eocene (ca. 49 Ma). We provide evidence that small increases in $\delta^{18}O$ values across five of the eight sequence boundaries (E2-E3, E4-E5, E5-E6, E7-E8, and E9-E10) are consistent with sea-level falls associated with the growth and decay of small ice sheets during a time period previously believed to have been ice free. Overall, the Bass River middle Eocene Shark River Formation record is relatively incomplete with long hiatuses (during a period of global cooling), compared to the lower Eocene Manasquan Formation and upper Eocene Absecon Inlet Formation, which record relatively continuous sedimentation with shorter hiatuses. A less-complete middle Eocene section also occurs in the Gulf Coast of the United States and in northwest Europe (Miller et al., 2005b) and may reflect a global response of margin sedimentation to higher-amplitude glacial sea-level fluctuations than in the early Eocene. The shallow setting of Bass River may have been influenced by freshwater input, though in general the amplitude and patterns of $\delta^{18}O$ changes are similar to those of deep-sea records (apart from the upper section of sequence E7), indicating minimal overprinting. Despite the difficulties associated with using New Jersey shelf sequence boundaries to understand the glacial influences on sea level (i.e., long hiatuses, potential for freshwater input), we demonstrate a clear need for future studies focused on glacial interactions in the early to middle Eocene. Both our regional water-depth studies and geochemical proxies suggest significant ice growth not only in the middle Eocene "doubthouse", but also in the early Eocene "greenhouse".

ACKNOWLEDGMENTS

We thank the International Ocean Discovery Program for supplying the Bass River core, Rutgers Core Repository for sampling, J.D. Wright and the Stable Isotope Laboratory in the Department of Earth and Planetary Sciences at Rutgers University for analyzing isotopes, and the Institute of

Marine and Coastal Sciences at Rutgers University for running Mg/Ca analyses. We also thank Mark Leckie, Peter McLaughlin, and an anonymous reviewer for substantially improving this manuscript.

REFERENCES CITED

Abbott, S.T., and Carter, R.M., 1994, The sequence architecture of mid-Pleistocene (0.35–0.95 Ma) cyclothems from New Zealand: Facies development during a period of known orbital control on sea-level cyclicity, *in* de Boer, P.L., and Smith, D.G., eds., Orbital Forcing and Cyclic Sequences: International Association of Sedimentologists Special Publication 19, p. 367–394.

Abreu, V.S., and Anderson, J.B., 1998, Glacial eustasy during the Cenozoic: Sequence stratigraphic implications: American Association of Petroleum Geologists Bulletin, v. 82, p. 1385–1400.

Anand, P., Elderfield, H., and Conte, M.H., 2003, Calibration of Mg/Ca thermometry in planktonic foraminifera from sediment trap time series: Paleoceanography, v. 18, 1050, https://doi.org/10.1029/2002PA000846.

Babila, T.L., Rosenthal, Y., Wright, J.D., and Miller, K.G., 2016, A continental shelf perspective of ocean acidification and temperature evolution during the Paleocene-Eocene Thermal Maximum: Geology, v. 44, p. 275–278, https://doi.org/10.1130/G37522.1.

Bandy, O.L., 1949, Eocene and Oligocene foraminifera from Little Stave Creek, Clarke County, Alabama: Bulletins of American Paleontology, v. 32, no. 131, p. 1–211.

Bandy, O.L., 1960, General correlation of foraminiferal structure with environment: International Geological Congress, 21st Session, Copenhagen, Reports, Pt. 22, p. 7–19.

Barker, P.F., Diekmann, B., and Escutia, C., 2007, Onset of Cenozoic Antarctic glaciation: Deep-Sea Research Part II: Topical Studies in Oceanography, v. 54, p. 2293–2307, https://doi.org/10.1016/j.dsr2.2007.07.027.

Birkenmajer, K., 1988, Tertiary glacial and interglacial deposits, South Shetland Islands, Antarctica: Geochronology versus biostratigraphy (a progress report): Polish Academy of Sciences Bulletin: Earth Science, v. 36, p. 133–145.

Boersma, A., 1984, Handbook of Common Tertiary *Uvigerina*: Stony Point, New York, Microclimates Press, 207 p.

Bohaty, S.M., and Zachos, J.C., 2003, Significant Southern Ocean warming event in the late middle Eocene: Geology, v. 31, p. 1017–1020, https://doi.org/10.1130/G19800.1.

Borrelli, C., Cramer, B.S., and Katz, M.E., 2014, Bipolar Atlantic deepwater circulation in the middle-late Eocene: Effects of Southern Ocean opening: Paleoceanography, v. 29, p. 308–327, https://doi.org/10.1002/2012PA002444.

Boulila, S., Galbrun, B., Miller, K.G., Pekar, S.F., Browning, J.V., Laskar, J., and Wright, J.D., 2011, On the origin of the Cenozoic and Mesozoic "third-order" eustatic sequences: Earth-Science Reviews, v. 109, p. 94–112, https://doi.org/10.1016/j.earscirev.2011.09.003.

Brown, L.F., and Fisher, W.L., 1977, Seismic-stratigraphic interpretation of depositional systems: Examples from Brazilian rift and pull-apart basins, *in* Payton, C.E., ed., Seismic Stratigraphy: Applications to Hydrocarbon Exploration: American Association of Petroleum Geologists Memoir 26, p. 213–248.

Browning, J.V., Miller, K.G., and Pak, D.K., 1996, Global implications of lower to middle Eocene sequence boundaries on the New Jersey coastal plain: The icehouse cometh: Geology, v. 24, no. 7, p. 639–642, https://doi.org/10.1130/0091-7613(1996)024<0639:GIOLTM>2.3.CO;2.

Browning, J.V., Miller, K.G., and Olsson, R.K., 1997a, Lower to middle Eocene benthic foraminiferal biofacies and lithostratigraphic units and their relationship to sequences, New Jersey Coastal Plain, *in* Miller, K.G., and Snyder, S.W., eds., Proceedings of the Ocean Drilling Program, Scientific Results, Volume 150X: College Station, Texas, Ocean Drilling Program, p. 207–228, https://doi.org/10.2973/odp.proc.sr.150X.333.1997.

Browning, J.V., Miller, K.G., Van Fossen, M., Liu, C., Pak, D.K., Aubry, M.-P., and Bybell, L.M., 1997b, Early to middle Eocene sequences of the New Jersey Coastal Plain and their significance for global climate change, *In* Miller, K.G., and Snyder, S.W., eds., Proceedings of the Ocean Drilling Program, Scientific Results, Volume 150X: College Station, Texas, Ocean Drilling Program, p. 229–242, https://doi.org/10.2973/odp.proc.sr.150X.315.1997.

Carter, A., Riley, T.R., Hillenbrand, C.-D., and Rittner, M., 2017, Widespread Antarctic glaciation during the Late Eocene: Earth and Planetary Science Letters, v. 458, p. 49–57, https://doi.org/10.1016/j.epsl.2016.10.045.

Charletta, A.C., 1980, Eocene benthic foraminiferal paleoecology and paleobathymetry of the New Jersey continental margin [Ph.D. thesis]: New Brunswick, New Jersey, Rutgers University, 84 p.

Christensen, B.A., Miller, K.G., and Olsson, R.K., 1995, Eocene-Oligocene benthic foraminiferal biofacies and depositional sequences at the ACGS #4 borehole, New Jersey coastal plain: Palaios, v. 10, p. 103–132, https://doi.org/10.2307/3515178.

Christie-Blick, N., and Driscoll, N.W., 1995, Sequence stratigraphy: Annual Review of Earth and Planetary Sciences, v. 23, p. 451–478, https://doi.org/10.1146/annurev.ea.23.050195.002315.

Cohen, A.S., 2003, Paleoecological archives in lake deposits 2: Records from important groups, *in* Paleolimnology: The History and Evolution of Lake Systems: Oxford, UK, Oxford University Press, p. 287–328.

Coxall, H.K., Wilson, P.A., Pälike, H., Lear, C.H., and Backman, J., 2005, Rapid stepwise onset of Antarctic glaciation and deeper calcite compensation in the Pacific Ocean: Nature, v. 433, p. 53–57, https://doi.org/10.1038/nature03135.

Cramer, B.S., Toggweiler, J.R., Wright, J.D., Katz, M.E., and Miller, K.G., 2009, Ocean overturning since the Late Cretaceous: Inferences from a new benthic foraminiferal isotope compilation: Paleoceanography, v. 24, PA4216, https://doi.org/10.1029/2008PA001683.

Cramer, B.S., Miller, K.G., Barrett, P.K., and Wright, J.D., 2011, Late Cretaceous–Neogene trends in deep ocean temperature and continental ice volume: Reconciling records of benthic foraminiferal geochemistry ($\delta^{18}O$ and Mg/Ca) with sea level history: Journal of Geophysical Research, v. 116, C12023, https://doi.org/10.1029/2011JC007255.

Culver, S.J., 1988, New foraminiferal depth zonation of the northwestern Gulf of Mexico: Palaios, v. 3, p. 69–85, https://doi.org/10.2307/3514545.

Davis, J.C., 2002, Statistics and Data Analysis in Geology: New York, John Wiley & Sons, Inc., 656 p.

Deck, L.T., 1985, Ostracodes of the Piney Point Formation, Pamunkey River, Virginia: Virginia Minerals, p. 186–191.

DeConto, R.M., and Pollard, D., 2003a, Rapid Cenozoic glaciation of Antarctica induced by declining atmospheric CO_2: Nature, v. 421, p. 245–249, https://doi.org/10.1038/nature01290.

DeConto, R.M., and Pollard, D., 2003b, A coupled climate–ice sheet modeling approach to the early Cenozoic history of the Antarctic ice sheet: Palaeogeography, Palaeoclimatology, Palaeoecology, v. 198, p. 39–52, https://doi.org/10.1016/S0031-0182(03)00393-6.

Douglas, R.G., 1979, Benthic foraminiferal ecology and paleoecology: A review of concepts and methods, *in* Lipps, J.H., Berger, W.H., Buzas, M.A., Douglas, R.G., and Ross, C.A., eds., Foraminiferal Ecology and Paleoecology: Society of Economic Paleontologists and Mineralogists Short Course Notes 6, p. 21–53, https://doi.org/10.2110/scn.79.06.0021.

Elderbak, K., and Leckie, R.M., 2016, Paleocirculation and foraminiferal assemblages of the Cenomanian–Turonian Bridge Creek Limestone bedding couplets: Productivity vs. dilution during OAE2: Cretaceous Research, v. 60, p. 52–77, https://doi.org/10.1016/j.cretres.2015.11.009.

Emiliani, C., 1955, Pleistocene temperatures: The Journal of Geology, v. 63, p. 538–578, https://doi.org/10.1086/626295.

Enright, R., Jr., 1969, The stratigraphy, micropaleontology, and paleoenvironmental analysis of the Eocene sediments of the New Jersey Coastal Plain [Ph.D. thesis]: New Brunswick, New Jersey, Rutgers University, 242 p.

Epstein, S., Buchsbaum, R., Lowenstam, H.A., and Hurey, H.C., 1953, Revised carbonate-water isotopic temperature scale: Geological Society of America Bulletin, v. 64, p. 1315–1326, https://doi.org/10.1130/0016-7606(1953)64[1315:RCITS]2.0.CO;2.

Evans, D., and Müller, W., 2012, Deep time foraminifera Mg/Ca paleothermometry: Nonlinear correction for secular change in seawater Mg/Ca: Paleoceanography, v. 27, PA4205, https://doi.org/10.1029/2012PA002315.

Exon, N.F., Kennett, J.P., and Malone, M.J., 2004, Leg 189 synthesis: Cretaceous–Holocene history of the Tasmanian gateway, *in* Exon, N.J., Kennett, J.P., and Malone, M.J., eds., Proceedings of the Ocean Drilling Program, Scientific Results, Volume 189: College Station, Texas, Ocean Drilling Program, p. 1–37, https://doi.org/10.2973/odp.proc.sr.189.101.2004.

Fairbanks, R.G., 1989, A 17,000-year glacio-eustatic sea level record: Influence of glacial melting rates on the Younger Dryas event and deep-ocean circulation: Nature, v. 342, p. 637–642, https://doi.org/10.1038/342637a0.

Fairbanks, R.G., and Matthews, R.K., 1978, The marine oxygen isotopic record in Pleistocene coral, Barbados, West Indies: Quaternary Research, v. 10, p. 181–196, https://doi.org/10.1016/0033-5894(78)90100-X.

Frenzel, P., and Boomer, I., 2005, The use of ostracodes from marginal marine, brackish waters as bioindicators of modern and Quaternary environmental change: Palaeogeography, Palaeoclimatology, Palaeoecology, v. 225, p. 68–92, https://doi.org/10.1016/j.palaeo.2004.02.051.

Geyer, W.R., Bearsley, R.C., Lentz, S.J., Candela, J., Limeburner, R., Johns, W.E., Castro, B.M., and Soares, I.D., 1996, Physical oceanography of the Amazon shelf: Continental Shelf Research, v. 16, p. 576–616.

Gibson, T.G., 1989, Planktonic benthonic foraminiferal ratios: Modern patterns and Tertiary applicability: Marine Micropaleontology, v. 15, p. 29–52, https://doi.org/10.1016/0377-8398(89)90003-0.

Gradstein, F.M., Ogg, J.G., Schmidtz, M.D., and Ogg, G.M., eds., 2012, The Geologic Time Scale: New York, Elsevier, 1144 p.

Gräfe, K.U., 1999, Foraminiferal evidence for Cenomanian sequence stratigraphy and palaeoceanography of the Boulonnais (Paris Basin, northern France): Palaeogeography, Palaeoclimatology, Palaeoecology, v. 153, p. 41–70, https://doi.org/10.1016/S0031-0182(99)00080-2.

Grimsdale, T.F., and van Morkhoven, F.P.C.M., 1955, The ratio between pelagic and benthonic foraminifera as a means of estimating depth of deposition of sedimentary rocks, *in* Proceedings of the Fourth World Petroleum Congress, Section I/D: Rome, Carlo Colombo, p. 474–491.

Guttman, L., 1954, Some necessary conditions for common factor analysis: Psychometrika, v. 19, p. 149–161, https://doi.org/10.1007/BF02289162.

Hammer, Ø., Harper, D.A.T., and Ryan, P.D., 2001, PAST: Paleontological statistics software package for education and data analysis: Palaeontologia Electronica, v. 4, no. 1, 4, https://palaeo-electronica.org/2001_1/past/issue1_01.htm.

Haq, B.U., Hardenbol, J., and Vail, P.R., 1987, Chronology of fluctuating sea levels since the Triassic (250 million years ago to Present): Science, v. 235, p. 1156–1167, https://doi.org/10.1126/science.235.4793.1156.

Harman, H.H., 1976, Modern Factor Analysis: Chicago, University of Chicago Press, 508 p.

Harris, A.D., Miller, K.M., Browning, J.V., Sugarman, P.J., Olsson, R.K., Cramer, B.S., and Wright, J.D., 2010, Integrated studies of Paleocene–lowermost Eocene sequences, New Jersey Coastal Plain: Evidence for glacioeustatic control: Paleoceanography, v. 25, PA3211, https://doi.org/10.1029/2009PA001800.

Hazel, J.E., 1968, Ostracodes from the Brightseat Formation (Danian) of Maryland: Journal of Paleontology, v. 42, p. 100–137.

Howe, H.V., 1939, Cook Mountain Eocene foraminifera: Louisiana Geological Survey Geological Bulletin 14, 122 p.

Imbrie, J., and Kipp, N.G., 1971, A new micropaleonotological method for quantitative paleoclimatology: Application to a late Pleistocene Caribbean core, *in* Turekian, K.K., ed., The Late Cenozoic Glacial Ages: New Haven, Connecticut, Yale University Press, p. 71–181.

Inglis, G.N., Farnsworth, A., Lunt D., Foster, G.L., Hollis, C.J., Pagani, M., Jardine, P.E., Pearson, P.N., Markwick, P., Galsworthy, A.M.J., Raynham, L., Taylor, K.W.R., and Pancost, R.D., 2015, Descent toward the Icehouse: Eocene sea surface cooling inferred from GDGT distributions: Paleoceanography, v. 30, p. 1000–1020, https://doi.org/10.1002/2014PA002723.

John, C.M., Karner, G.D., and Mutti, M., 2004, $\delta^{18}O$ and Marion Plateau backstripping: Combining two approaches to constrain late middle Miocene eustatic amplitude: Geology, v. 32, p. 829–832, https://doi.org/10.1130/G20580.1.

John, C.M., Karner, G.D., Browning, E., Leckie, M., Mateo, Z., Carson, B., and Lowery, C., 2011, Timing and magnitude of Miocene eustasy derived from the mixed siliciclastic-carbonate stratigraphic record of the northeastern Australian margin: Earth and Planetary Science Letters, v. 304, p. 455–467, https://doi.org/10.1016/j.epsl.2011.02.013.

Jones, G.D., 1983, Foraminiferal biostratigraphy and depositional history of the Middle Eocene rocks of the coastal plain of North Carolina: North Carolina Geological Survey Special Publication 8, 80 p.

Jorissen, F.J., Wittling, I., Peypouquet, J.P., Rabouille, C., and Relexans, J.C., 1998, Live benthic foraminiferal faunas off Cape Blanc, NW-Africa: Community structure and microhabitats: Deep-Sea Research Part I: Oceanographic Research Papers, v. 45, p. 2157–2188, https://doi.org/10.1016/S0967-0637(98)00056-9.

Katz, M.E., and Miller, K.G., 1991, Early Paleogene benthic foraminiferal assemblages and stable isotopes in the Southern Ocean, *in* Ciesielski, P.F., Kristofferson, Y., et al., Proceedings of the Ocean Drilling Program, Scientific Results, Volume 114: College Station, Texas, Ocean Drilling Program, p. 481–512, https://doi.org/10.2973/odp.proc.sr.114.147.1991.

Katz, M.E., and Miller, K.G., 1996, Eocene to Miocene oceanographic and provenance changes in a sequence stratigraphic framework: Benthic foraminifers of the New Jersey Margin, *in* Mountain, G.S., Miller, K.G., Blum, P., Poag, C.W., and Twichell, D.C., eds., Proceedings of the Ocean Drilling Program, Scientific Results, Volume 150: College Station, Texas, Ocean Drilling Program, p. 65–95, https://doi.org/10.2973/odp.proc.sr.150.003.1996.

Katz, M.E., Miller, K.G., and Mountain, G.S., 2003a, Biofacies and lithofacies evidence for paleoenvironmental interpretations of upper Neogene sequences on the New Jersey continental shelf (ODP Leg 174A), *in* Olson, H.C., and Leckie, R.M., eds., Micropaleontologic Proxies for Sea-Level Change and Stratigraphic Discontinuities: SEPM (Society for Sedimentary Geology) Special Publication 75, p. 131–146, https://doi.org/10.2110/pec.03.75.0131.

Katz, M.E., Tjalsma, R.C., and Miller, K.G., 2003b, Oligocene bathyal to abyssal benthic foraminifera of the Atlantic Ocean: Micropaleontology, v. 49, suppl. 2, 45 p.

Katz, M.E., Katz, D.R., Wright, J.D., Miller, K.G., Pak, D.K., Shackleton, N.J., and Thomas, E., 2003c, Early Cenozoic benthic foraminiferal isotopes: Species reliability and interspecies correction factors: Paleoceanography, v. 18, 1024, https://doi.org/10.1029/2002PA000798.

Katz, M.E., Miller, K.G., Wright, J.D., Wade, B.S., Browning, J.V., Cramer, B.S., and Rosenthal, Y., 2008, Stepwise transition from the Eocene greenhouse to the Oligocene icehouse: Nature Geoscience, v. 1, p. 329–334, https://doi.org/10.1038/ngeo179.

Katz, M.E., Cramer, B.S., Franzese, A., Hönisch, B., Miller, K.G., Rosenthal, Y., and Wright, J.D., 2010, Traditional and emerging geochemical proxies in foraminifera: Journal of Foraminiferal Research, v. 40, p. 165–192, https://doi.org/10.2113/gsjfr.40.2.165.

Katz, M.E., Browning, J.V., Miller, K.G., Monteverde, D., Mountain, G.S., and Williams, R.H., 2013, Paleobathymetry and sequence stratigraphic interpretations from benthic foraminifera: Insights on New Jersey shelf architecture, IODP Expedition 313: Geosphere, v. 9, p. 1488–1513, https://doi.org/10.1130/GES00872.1.

Kennett, J.P., and Shackleton, N.J., 1976, Oxygen isotopic evidence for the development of the psychrosphere 38 Myr ago: Nature, v. 260, p. 513–515, https://doi.org/10.1038/260513a0.

Kennett, J.P., and Stott, L.D., 1990, Proteus and Proto-Oceanus: Ancestral Paleogene oceans as revealed from Antarctic stable isotopic results: ODP Leg 113, *in* Barber, P.F., Kennett, J.P., et al., Proceedings of the Ocean Drilling Program, Scientific Results, Volume 113: College Station, Texas, Ocean Drilling Program, p. 865–880, https://doi.org/10.2973/odp.proc.sr.113.188.1990.

Kominz, M.A., Miller, K.G., and Browning, J.V., 1998, Long-term and short-term global Cenozoic sea-level estimates: Geology, v. 26, p. 311–314, https://doi.org/10.1130/0091-7613(1998)026<0311:LTASTG>2.3.CO;2.

Kominz, M.A., Browning, J.V., Miller, K.G., Sugarman, P.J., Misintseva, S., and Scotese, C.R., 2008, Late Cretaceous to Miocene sea-level estimates from the New Jersey and Delaware coastal plain coreholes: An error analysis: Basin Research, v. 20, p. 211–226, https://doi.org/10.1111/j.1365-2117.2008.00354.x.

Krutak, P.R., 1961, Jackson Eocene Ostracoda from the Cocoa Sand of Alabama: Journal of Paleontology, v. 35, p. 769–788.

Kump, L.R., and Arthur, M.A., 1999, Interpreting carbon-isotope excursions: Carbonates and organic matter: Chemical Geology, v. 161, p. 181–198, https://doi.org/10.1016/S0009-2541(99)00086-8.

Lanci, L., Kent, D.V., and Miller, K.G., 2002, Detection of Late Cretaceous and Cenozoic sequence boundaries on the Atlantic coastal plain using core log integration of magnetic susceptibility and natural gamma ray measurements at Ancora, New Jersey: Journal of Geophysical Research, v. 107, 2216, https://doi.org/10.1029/2000JB000026.

Lear, C.H., Elderfield, H., and Wilson, P.A., 2000, Cenozoic deep-sea temperatures and global ice volumes from Mg/Ca in benthic foraminiferal calcite: Science, v. 287, p. 269–272, https://doi.org/10.1126/science.287.5451.269.

Lear, C.H., Rosenthal, Y., and Slowey, N., 2002, Benthic foraminiferal Mg/Ca-paleothermometry: A revised core-top calibration: Geochimica et Cosmochimica Acta, v. 66, p. 3375–3387, https://doi.org/10.1016/S0016-7037(02)00941-9.

Lear, C.H., Bailey, T.R., Pearson, P.H., Coxall, H.K., and Rosenthal, Y., 2008, Cooling and ice-sheet growth across the Eocene-Oligocene transition: Geology, v. 36, p. 251–254, https://doi.org/10.1130/G24584A.1.

Leckie, R.M., and Olson, H.C., 2003, Foraminifera as proxies for sea-level change on siliciclastic margins, *in* Olson, H.C., and Leckie, R.M., eds., Micropaleontologic Proxies for Sea-Level Change and Stratigraphic Discontinuities: SEPM (Society for Sedimentary Geology) Special Publication 75, p. 5–19, https://doi.org/10.2110/pec.03.75.0005.

Levanter, A., Williams, D.F., and Kennet, J.P., 1982, Dynamics of the Laurentide ice sheet during the last glaciation: Evidence from the Gulf of Mexico: Earth and Planetary Science Letters, v. 59, p. 11–17, https://doi.org/10.1016/0012-821X(82)90112-1.

Livermore, R., Hillenbrand, C.-D., Meredith, M., and Eagles, G., 2007, Drake Passage and Cenozoic climate: An open and shut case?: Geochemistry Geophysics Geosystems, v. 8, Q01005, https://doi.org/10.1029/2005GC001224.

Loutit, T.S., Hardenbol, J., Vail, P.R., and Baum, G.R., 1988, Condensed section: The key to age determination and correlation of continental margin sequences, *in* Wilgus, C.K., Hastings, B.S., Kendall, C.G.St.C., Posamentier, H.W., Ross, C.A., and Van Wagoner, J.C., eds., Sea-Level Changes: An Integrated Approach: Society of Economic Paleontologists and Mineralogists Special Publication 42, p. 183–213, https://doi.org/10.2110/pec.88.01.0183.

Lynch-Stieglitz, J., Curry, W.B., and Slowey, N., 1999, A geostrophic transport estimate for the Florida Current from the oxygen isotope composition of benthic foraminifera: Paleoceanography, v. 14, p. 360–373, https://doi.org/10.1029/1999PA900001.

Mackensen, A., Schumacher, S., Radke, J., and Schmidt, D.N., 2000, Microhabitat preferences and stable carbon isotopes of endobenthic foraminifera: Clue to quantitative reconstruction of oceanic new production?: Marine Micropaleontology, v. 40, p. 233–258, https://doi.org/10.1016/S0377-8398(00)00040-2.

Magurran, A.E., 1988, Ecological Diversity and Its Measurement: Princeton, New Jersey, Princeton University Press, 179 p., https://doi.org/10.1007/978-94-015-7358-0.

Mendes, I., Gonzalez, R., Dias, J.M.A., Lobo, F., and Martins, V., 2004, Factors influencing recent benthic foraminifera distribution on the Guadiana shelf (Southwestern Iberia): Marine Micropaleontology, v. 51, p. 171–192, https://doi.org/10.1016/j.marmicro.2003.11.001.

Miller, K.G., and Katz, M.E., 1987, Eocene benthic foraminiferal biofacies of the New Jersey Transect, *in* Poag C.W., Watts, A.B., et al., Initial Reports of the Deep Sea Drilling Project, Volume 95: Washington, D.C., U.S. Government Printing Office, 267–298, https://doi.org/10.2973/dsdp.proc.95.107.1987.

Miller, K.G., and Mountain, G.S., 1994, Global sea-level change and the New Jersey margin, *in* Mountain, G.S., Miller, K.G., Blum, P., et al., Proceedings of the Ocean Drilling Program, Initial Reports, Volume 150: College Station, Texas, Ocean Drilling Program, p. 11–20, https://doi.org/10.2973/odp.proc.ir.150.102.1994.

Miller, K.G., Wright, J.D., and Fairbanks, R.G., 1991, Unlocking the Ice House: Oligocene-Miocene oxygen isotopes, eustasy, and margin erosion: Journal of Geophysical Research, v. 96, p. 6829–6848, https://doi.org/10.1029/90JB02015.

Miller, K.G., Mountain, G.S., Browning, J.V., Kominz, M., Sugarman, P.J., Christie-Blick, N., Katz, M.E., and Wright, J.D., 1998a, Cenozoic global sea level, sequences, and the New Jersey Transect: Results from coastal plain and continental slope drilling: Reviews of Geophysics, v. 36, p. 569–601, https://doi.org/10.1029/98RG01624.

Miller, K.G., Sugarman, P.J., Browning, J.V., Olsson, R.K., Pekar, S.F., Reilly, T.J., Cramer, B.S., Aubry, M.-P., Lawrence, R.P., Curran, J., Stewart, M., Metzger, J.M., Uptegrove, J., Bukry, D., Burckle, L.H., Wright, J.D., Feigenson, M.D., Brenner, G.J., and Dalton, R.F., 1998b, Bass River site, *in* Miller, K.G., Sugarman, P.J., Browning, J.V., et al., Proceedings of the Ocean Drilling Program, Initial Reports, Volume 174AX: College Station, Texas, Ocean Drilling Program, p. 5–43, https://doi.org/10.2973/odp.proc.ir.174AX.101.1998.

Miller, K.G., Sugarman, P.J., Browning, J.V., Kominz, M.A., Olsson, R.K., Feigenson, M.D., and Hernandez, J.C., 2004, Upper Cretaceous sequences and sea-level history, New Jersey Coastal Plain: Geological Society of America Bulletin, v. 116, p. 368–393, https://doi.org/10.1130/B25279.1.

Miller, K.G., Kominz, M.A., Browning, J.V., Wright, J.D., Mountain, G.S., Katz, M.E., Sugarman, P.J., Cramer, B.S., Christie-Blick, N., and Pekar, S.F., 2005a, The Phanerozoic record of global sea-level change: Science, v. 310, p. 1293–1298, https://doi.org/10.1126/science.1116412.

Miller, K.G., Wright, J.D., and Browning, J.V., 2005b, Visions of ice sheets in a greenhouse world: Marine Geology, v. 217, p. 215–231, https://doi.org/10.1016/j.margeo.2005.02.007.

Miller, K.G., Wright, J.D., Katz, M.E., Browning, J.V., Cramer, B.S., Wade, B.S., and Mizintseva, S.F., 2008, A view of Antarctic ice-sheet evolution from sea-level and deep-sea isotope changes during the Late Cretaceous–Cenozoic, *in* Cooper, A., Raymond, C., and ISAES Editorial Team, eds., Antarctica: A Keystone in a Changing World—Online Proceedings for the Tenth International Symposium on Antarctic Earth Sciences: U.S. Geological Survey Open-File Report 2007-1047, p. 55–70, https://doi.org/10.3133/ofr20071047KP06.

Miller, K.G., Mountain, G.S., Wright, J.D., and Browning, J.V., 2011, A 180-million-year record of sea level and ice volume variations from continental margin and deep-sea isotopic records: Oceanography (Washington, D.C.), v. 24, p. 40–53, https://doi.org/10.5670/oceanog.2011.26.

Miller, K.G., Wright, J.D., Browning, J.V., Kulpecz, A., Kominz, M., Naish, T.R., Cramer, B.S., Rosenthal, Y., Peltier, W.R., and Sosdian, S., 2012, High tide of the warm Pliocene: Implications of global sea level for Antarctic deglaciation: Geology, v. 40, p. 407–410, https://doi.org/10.1130/G32869.1.

Moucha, R., Forte, A.M., Mitrovica, J.X., Rowley, D.B., Quéré, S., Simmons, N.A., and Grand, S.P., 2008, Dynamic topography and long-term sea level variations: There is no such thing as a stable continental platform: Earth and Planetary Science Letters, v. 271, p. 101–108, https://doi.org/10.1016/j.epsl.2008.03.056.

Natland, M.L., 1933, The temperature and depth distribution of some recent and fossil foraminifera in the southern California region: Bulletin of the Scripps Institution of Oceanography: Technical Series, v. 3, p. 225–230.

Neal, J., and Abreu, V., 2009, Sequence stratigraphy hierarchy and the accommodation succession method: Geology, v. 37, p. 779–782, https://doi.org/10.1130/G25722A.1.

Nguyen, T.M.P., Petrizzo, M.R., and Speijer, R.P., 2009, Experimental dissolution of a fossil foraminiferal assemblage (Paleocene-Eocene Thermal Maximum, Dababiya, Egypt): Implications for Paleoenvironmental reconstructions: Marine Micropaleontology, v. 73, p. 241–258, https://doi.org/10.1016/j.marmicro.2009.10.005.

New Jersey Geological Survey, 1990, Generalized stratigraphic table for New Jersey and Delaware: New Jersey Geological Survey Information Circular 1.

Olsson, R.K., and Wise, S.W., Jr., 1987, Upper Paleocene to middle Eocene depositional sequences and hiatuses in the New Jersey Atlantic Margin, *in* Ross, C.A., and Haman, D., eds., Timing and Depositional History of Eustatic Sequences: Constraints on Seismic Stratigraphy: Cushman Foundation of Foraminiferal Research Special Publication 24, p. 99–112.

Owens, J.P., Bybell, L.M., Paulachok, G., Ager, T.A., Gonzalez, V.M., and Sugarman, P.J., 1988, Stratigraphy of the Tertiary sediments in a 945-foot-deep corehole near Mays Landing in the southeastern New Jersey coastal plain: U.S. Geological Survey Professional Paper 1484, 39 p.

Pagani, M., Zachos, J.C., Freeman, K.H., Tipple, B., and Bohaty, S., 2005, Marked decline in atmospheric carbon dioxide concentrations during the Paleogene: Science, v. 309, p. 600–603, https://doi.org/10.1126/science.1110063.

Pagani, M., Huber, M., Liu, Z., Bohaty, S.M., Henderiks, J., Sijp, W., Krishnan, S., and DeConto, R.M., 2011, The role of carbon dioxide during the onset of Antarctic glaciation: Science, v. 334, p. 1261–1264, https://doi.org/10.1126/science.1203909.

Passlow, V., 1997, Quaternary ostracods as palaeoceanographic indicators: A case study off southern Australia: Palaeogeography, Palaeoclimatology, Palaeoecology, v. 131, p. 315–325, https://doi.org/10.1016/S0031-0182(97)00009-6.

Patterson, R.T., and Kumar, A., 2000, Use of Arcellacea (Thecamoebians) to gauge levels of contamination and remediation in industrially polluted lakes, *in* Martin, R.E., ed., Environmental Micropaleontology: The Application of Microfossils to Environmental Geology: New York, Kluwer Academic/Plenum Publishers, Topics in Geobiology, v. 15, p. 257–278.

Pearson, P.N., Foster, G.L., and Wade, B.S., 2009, Atmospheric carbon dioxide through the Eocene-Oligocene transition: Nature, v. 461, p. 1110–1113, https://doi.org/10.1038/nature08447.

Pekar, S.F., and Kominz, M.L., 2001, Benthic foraminiferal biofacies water depth estimates from the onshore New Jersey Oligocene strata using a two-dimensional paleoslope model: Journal of Sedimentary Research, v. 71, p. 608–620, https://doi.org/10.1306/100600710608.

Pekar, S.F., Miller, K.G., and Browning, J.V., 1997, New Jersey Coastal Plain Oligocene sequences, *in* Miller, K.G., and Snyder, S.W., Proceedings of the Ocean Drilling Program, Scientific Results, Volume 150X: College Station, Texas, Ocean Drilling Program, p. 187–206, https://doi.org/10.2973/odp.proc.sr.150X.314.1997.

Pekar, S.F., Christie-Blick, N., Kominz, M.A., and Miller, K.G., 2002, Calibration between eustatic estimates from backstripping and oxygen isotopic records for the Oligocene: Geology, v. 30, p. 903–906, https://doi.org/10.1130/0091-7613(2002)030<0903:CBEEFB>2.0.CO;2.

Pekar, S.F., Christie-Blick, N., Miller, K.G., and Kominz, M.A., 2003, Quantitative constraints on the origin of stratigraphic architecture at passive continental margins: Oligocene sedimentation in New Jersey, U.S.A.: Journal of Sedimentary Research, v. 73, p. 227–245, https://doi.org/10.1306/090402730227.

Peryt, D., Lahodynsky, R., and Durakiewicz, T., 1997, Deep-water agglutinated foraminiferal changes and stable isotope profiles across the Cretaceous-Paleogene boundary in the Rotwandgraben section, Eastern Alps (Austria): Palaeogeography, Palaeoclimatology, Palaeoecology, v. 132, p. 287–307, https://doi.org/10.1016/S0031-0182(97)00056-4.

Poag, C.W., 1981, Ecologic Atlas of Benthic Foraminifera of the Gulf of Mexico: Woods Hole, Massachusetts, Marine Science International, 174 p.

Posamentier, H.W., and Vail, P.R., 1988, Eustatic controls on clastic deposition II—Sequence and systems tract models, *in* Wilgus, C.K., Hastings, B.S., Kendall, C.G.St.C., Posamentier, H.W., Ross, C.A., and Van Wagoner, J.C., eds., Sea-Level Changes: An Integrated Approach: Society of Economic Paleontologists and Mineralogists Special Publication 42, p. 125–154, https://doi.org/10.2110/pec.88.01.0125.

Posamentier, H.W., Jervey, M.Y., and Vail, P.R., 1988, Eustatic controls on clastic deposition I—Conceptual framework, *in* Wilgus, C.K., Hastings, B.S., Kendall, C.G.St.C., Posamentier, H.W., Ross, C.A., and Van Wagoner, J.C., eds., Sea-Level Changes: An Integrated Approach: Society of Economic Paleontologists and Mineralogists Special Publication 42, p. 109–124, https://doi.org/10.2110/pec.88.01.0109.

Roe, H.M., and Patterson, R.T., 2014, Arcellacea (testate amoebae) as bio-indicators of road salt contamination in lakes: Microbial Ecology, v. 68, p. 299–313, https://doi.org/10.1007/s00248-014-0408-3.

Rohling, E.J., and Cooke, S., 1999, Stable oxygen and carbon isotope ratios in foraminiferal carbonate, *in* Sen Gupta, B.K., ed., Modern Foraminifera: Dordrecht, Netherlands, Kluwer Academic, p. 239–258, https://doi.org/10.1007/0-306-48104-9_14.

Rosenthal, Y., Boyle, E.A., and Slowey, N., 1997, Temperature control on the incorporation of magnesium, strontium, fluorine, and cadmium into benthic foraminiferal shells from Little Bahama Bank: Prospects for thermocline paleoceanography: Geochimica et Cosmochimica Acta, v. 61, p. 3633–3643, https://doi.org/10.1016/S0016-7037(97)00181-6.

Rosenthal, Y., Field, M.P., and Sherrell, R.M., 1999, Precise determination of element/calcium ratios in calcareous samples using sector field inductively coupled plasma mass spectrometry: Analytical Chemistry, v. 71, p. 3248–3253, https://doi.org/10.1021/ac981410x.

Rowley, D.B., Forte, A.M., Moucha, R., Mitrovica, J.X., Simmons, N.A., and Grand, S.P., 2013, Dynamic topography change of the eastern United States since 3 million years ago: Science, v. 340, p. 1560–1563, https://doi.org/10.1126/science.1229180.

Scher, H.D., and Martin, E.E., 2006, Timing and climatic consequences of the opening of Drake Passage: Science, v. 312, p. 428–430, https://doi.org/10.1126/science.1120044.

Scher, H.D., Bohaty, S.M., Smith, B.W., and Munn, G.H., 2014, Isotopic interrogation of a suspected late Eocene glaciation: Paleoceanography, v. 29, p. 628–644, https://doi.org/10.1002/2014PA002648.

Sen Gupta, B.K., 1999, Foraminifera in marginal marine environments, *in* Sen Gupta, B.K., ed., Modern Foraminifera: Dordrecht, The Netherlands, Kluwer Academic Publishers, p. 141–159, https://doi.org/10.1007/0-306-48104-9_9.

Shackleton, N.J., 1967, Oxygen isotope analyses and Pleistocene temperatures reassessed: Nature, v. 215, p. 15–17, https://doi.org/10.1038/215015a0.

Shackleton, N.J., 1974, Attainment of isotopic equilibrium between ocean water and the benthic foraminifera genus *Uvigerina*: Isotopic changes in the ocean during the last glacial, *in* Labeyrie, J., ed., Les Méthodes Quantitatives d'Étude des Variations du Climat au Cours du Pléistocène: Colloques Internationaux de CNRS 219, p. 203–209.

Shackleton, N.J., Hall, M.A., and Vincent, E., 2000, Phase relationships between millennial-scale events 64,000–24,000 years ago: Paleoceanography, v. 15, p. 565–569, https://doi.org/10.1029/2000PA000513.

Stassen, P., Thomas, E., and Speijer, R.P., 2015, Paleocene-Eocene Thermal Maximum environmental change in the New Jersey Coastal Plain: Benthic foraminiferal biotic events: Marine Micropaleontology, v. 115, p. 1–23, https://doi.org/10.1016/j.marmicro.2014.12.001.

Steckler, M.S., Mountain, G.S., Miller, K.G., and Christie-Blick, N., 1999, Reconstruction of Tertiary progradation and clinoform development on the New Jersey passive margin by 2-D backstripping: Marine Geology, v. 154, p. 399–420, https://doi.org/10.1016/S0025-3227(98)00126-1.

Stickley, C.E., Brinkhuis, H., Schellenberg, S.A., Sluijs, A., Röhl, U., Fuller, M., Grauert, M., Huber, M., Warnaar, J., and Williams, G.L., 2004, Timing and nature of the deepening of the Tasmanian Gateway: Paleoceanography, v. 19, PA4027, https://doi.org/10.1029/2004PA001022.

Streeter, S.S., and Lavery, S.A., 1982, Holocene and latest glacial benthic foraminifera from the slope and rise off eastern North America: Geological Society of America Bulletin, v. 93, p. 190–199, https://doi.org/10.1130/0016-7606(1982)93<190:HALGBF>2.0.CO;2.

Swain, F.M., 1951, Ostracodes from wells in North Carolina: Part 1, Cenozoic Ostracoda: U.S. Geological Survey Professional Paper 234-A, 55 p.

Thomas, E., 1990, Late Cretaceous through Neogene deep-sea benthic foraminifers (Maud Rise, Weddell Sea, Antarctica), *in* Barker, P.F., Kennett, J.P., et al., Proceedings of the Ocean Drilling Program, Scientific Results, Volume 113: College Station, Texas, Ocean Drilling Program, p. 571–594, https://doi.org/10.2973/odp.proc.sr.113.123.1990.

Tjalsma, R.C., and Lohmann, G.P., 1983, Paleocene-Eocene bathyal and abyssal benthic foraminifera from the Atlantic Ocean: New York, Micropaleontology Press, Micropaleontology Special Publication 4, 90 p.

Trauth, M.H., Gebbers, R., and Marwan, N., 2010, MATLAB Recipes for Earth Sciences (third edition): Berlin, Springer-Verlag, 336 p., https://doi.org/10.1007/978-3-642-12762-5.

Vail, P.R., 1987, Seismic stratigraphy interpretation using sequence stratigraphy, Part 1: Seismic stratigraphy interpretation procedure, *in* Bally, A.W., ed., Atlas of Seismic Stratigraphy: American Association of Petroleum Geologists Studies in Geology 27, v. 1, p. 1–10.

Vail, P.R., Mitchum, R.M., Jr., Todd, R.G., Widmier, J.M., Thompson, S., III, Sangree, J.B., Bubb, J.N., and Hatlelid, W.G., 1977, Seismic stratigraphy and global changes of sea level, *in* Payton, C.E., ed., Seismic Stratigraphy—Applications to Hydrocarbon Exploration: American Association of Petroleum Geologists Memoir 26, p. 49–212.

Vail, P.R., Audemard, F., Bowman, S.A., Eisner, P.N., and Perez-Cruz, C., 1991, The stratigraphic signatures of tectonics, eustasy and sedimentology—An overview, *in* Einsele, G., Ricken, W., and Seilacher, A., eds., Cycles and Events in Stratigraphy: Berlin, Springer-Verlag, p. 617–659.

van der Zwaan, G.J., Jorissen, F.J., and de Stigter, H.C., 1990, The depth dependency of planktonic/benthic foraminiferal ratios: Constraints and applications: Marine Geology, v. 95, p. 1–16, https://doi.org/10.1016/0025-3227(90)90016-D.

van Morkhoven, F.P.C.M., Berggren, W.A., Edwards, A.S., et al., 1986, Cenozoic Cosmopolitan Deep-Water Benthic Foraminifera: Pau, France, Elf-Aquitaine, Memoire 11, 421 p.

Van Wagoner, J.C., Mitchum, R.M., Jr., Posamentier, H.W., and Vail, P.R., 1987, Seismic stratigraphy interpretation using sequence stratigraphy, Part 2: Key definitions of sequence stratigraphy, *in* Bally A.W., ed., Atlas of Seismic Stratigraphy: American Association of Petroleum Geologists Studies in Geology 27, v. 1, p. 11–14.

Van Wagoner, J.C., Posamentier, H.W., Mitchum, R.M., Vail, P.R., Sarg, J.F., Loutit, T.S., and Hardenbol, J., 1988, An overview of the fundamentals of sequence stratigraphy and key definitions, *in* Wilgus, C.K., Hastings, B.S., Kendall, C.G.St.C., Posamentier, H.W., Ross, C.A., and Van Wagoner, J.C., eds., Sea-Level Changes: An Integrated Approach: Society of Economic Paleontologists and Mineralogists Special Publication 42, p. 39–45, https://doi.org/10.2110/pec.88.01.0039.

Villa, G., Fioroni, C., Persico, D., Roberts, A.P., and Florindo, F., 2013, Middle Eocene to Late Oligocene Antarctic glaciation/deglaciation and Southern Ocean productivity: Paleoceanography, v. 29, p. 223–237, https://doi.org/10.1002/2013PA002518.

Weimer, P., and Posamentier, H.W., eds., 1993, Siliciclastic Sequence Stratigraphy: Recent Developments and Applications: American Association of Petroleum Geologists Memoir 58, 492 p.

Whatley, R.C., 1988, Ostracoda and palaeogeography, *in* De Deckler, P., Colin, J-P., and Peypouguet, J-P., eds., Ostracoda in the Earth Sciences: Elsevier, New York, p. 103–124.

Winn, R.D., Jr., Roberts, H.H., Kohl, B., Fillon, R.H., Bouma, A.H., and Constans, R.E., 1995, Latest Quaternary deposition on the outer shelf, northern Gulf of Mexico: Facies and sequence stratigraphy from Main Pass Block 303 shallow core: Geological Society of America Bulletin, v. 107, p. 851–866, https://doi.org/10.1130/0016-7606(1995)107<0851:LQDOTO>2.3.CO;2.

Winnick, M.J., and Caves, J.K., 2015, Oxygen isotope mass-balance constraints on Pliocene sea level and East Antarctic Ice Sheet stability: Geology, v. 43, p. 879–882, https://doi.org/10.1130/G36999.1.

Yasuhara, M., Hunt, G., Cronin, T.M., Hokanishi, N., Kawahata, H., Tsujimoto, A., and Ishitake, M., 2012, Climate forcing of Quaternary deep-sea benthic communities in the North Pacific Ocean: Paleobiology, v. 38, p. 162–179, https://doi.org/10.1017/S0094837300000464.

Zachos, J.C., Quinn, T.M., and Salamy, K.A., 1996, High-resolution (10^4 years) deep-sea foraminiferal stable isotope records of the Eocene-Oligocene climate transition: Paleoceanography, v. 11, p. 251–266, https://doi.org/10.1029/96PA00571.

Zachos, J., Pagani, M., Sloan, L., Thomas, E., and Billups, K., 2001, Trends, rhythms, and aberrations in global climate 65 Ma to present: Science, v. 292, p. 686–693, https://doi.org/10.1126/science.1059412.